Title
The Function of SATB2 in Neurodevelopment and Disease

Author
Finn, Thomas Sean

Publication Date
2023

Peer reviewed|Thesis/dissertation

UNIVERSITY OF CALIFORNIA
SANTA CRUZ

The function of Satb2 in neurodevelopment and disease

A dissertation submitted in partial satisfaction
of the requirements for the degree of

DOCTOR OF PHILOSOPHY

in

CHEMISTRY

by

Thomas Sean Finn

September 2023

The Dissertation of Thomas Sean Finn
is approved:

_____
Professor Bin Chen, chair

_____
Professor John MacMillan

_____
Professor Glenn Millhauser

_____
Professor Bradley Colquitt

_____
Peter Biehl
Vice Provost and Dean of Graduate Studies

Table of Contents

List of Figures

Abstract

The function of Satb2 in neurodevelopment and disease

Thomas Sean Finn

SATB2-Associated Syndrome (SAS) is a recently described disease characterized by developmental delay, severe intellectual deficiency, and behavioral problems. It is caused by heterozygous *de novo* mutations in the *SATB2* gene, which encodes a DNA-binding protein involved in chromatin remodeling, and often leads to loss-of-function. In the brain, SATB2 expression is mostly restricted to the projection neurons in the cerebral cortex and hippocampus, suggesting the etiology of SAS is likely defects in these neurons. In mice, Satb2 is required for specifying the subtype identities of callosal and subcerebral neurons. In the absence of *Satb2*, callosal neurons are mis-specified, and the subcerebral neurons are missing. However, prior studies on Satb2 function in brain development were performed using homozygous mutant mice. It remained to be determined how heterozygous loss-of-function of *SATB2*, as commonly seen in SAS patients, affects brain development.

Satb2$^{+/-}$ mice show consistent defects in cortical projection neurons and their axons. Single cell RNA-seq of postnatal day 28 *Satb2*$^{+/+}$, *Satb2*$^{+/-}$, and *Satb2 cko* cortices, shows many genes are mis-regulated in the *Satb2*$^{+/-}$ projection neurons. However, the downstream targets of Satb2 that mediate its functions in cortical neuron development and axon targeting have not been identified. This thesis reviews the function of Satb2 in cortical development and determines mechanisms of Satb2 in organizing higher-order chromatin structure, regulating the development of cortical projection neuron subtypes, and identifies the downstream target genes that mediate the function of Satb2. These findings elucidate fundamental mechanisms of cortical development and illuminate the etiology of SAS, facilitating the development of potential treatment strategies.

Acknowledgements

Bin, you have been such a wonderful mentor. You brought me on during a rough time in graduate school and gave me a home. I will always be grateful for your guidance, leadership, and tough love. Without your support, I would be lost.

Glen Millhauser, John MacMillan, and Bradley Colquitt for being on my thesis committee and providing me guidance and advice. Your constant positivity and support helped me through this journey. Euiseok Kim and Dave Feldheim for being awesome floor-mates and always being up for a good joke, laugh, or solid advice. Karen Meece for fielding all my random questions, keeping me on track, making sure I always had a TAship when I needed one, and good vent sessions. Jeremy Lee, for always believing in me and giving me my first taste of research. From the early Alzheimer's journal club days, to setting up lab space and building a team, to numerous beers, advice, and letters of rec, I really would not be here without you.

Jeremiah Tsyporin, my co-author, we've really been through it. Through the highs and lows, there's no one else I'd rather have on my team, trudging through the trenches. My lab mate Xiaoyi Guo, the double doctor. You were always a breath of fresh air when work got tough and you always made my day better. Alex Esparza, your enthusiasm and work ethic are unmatched. It's been my privilege to be your mentor in your transition into graduate school, I know you'll do great things. Gabby Servito for being a great lab mate and always being down for a laugh. And Charlene Guo for all your help and hard work during this last summer.

Hannah Maul-Newby-Brueckner for being such a great friend, and dog-Aunt, throughout graduate school; it would not have been the same without you. I'm glad we were able to trauma-bond during graduate school and I can't wait to see what your future holds.

Austin Kress, for being my friend and brother for the last decade. It's been a privilege growing up with you, traveling the world with you, and enduring the good times and the bad. I look up to you in so many ways, except height, and I look forward to many more years with you in my life.

I'd also like to thank my parents, Brian and Marcia, and my sister Kelly for supporting me and always being there no matter what. I really could not have done this without you, I love you all. To all my friends I have made over the years that I have not mentioned here. It's been a wild ride and you all make it worth it.

And lastly, to my dog Ham. Your undying optimism, love, and giant grin kept me sane these last few years.

The text of this dissertation includes a draft of the following manuscript in preparation for submission, written by both Thomas S Finn and Jeremiah Tsyporin:

***Satb2* haploinsufficiency results in an altered chromatin landscape, aberrant IT neuronal projections, and human disease**

Thomas S. Finn[1,*], Jeremiah Tsyporin[2,*], Sherry Wu[3,4], Min Dai[3,4], Xiaokuang Ma[5], Antoine Nehme[5], Sol Katzman[2] Austin Schubert[2], Shenfeng Qiu[5], Gord Fishell[3,4], Bin Chen[2,6,#]

[1] Department of Chemistry and Biochemistry, University of California Santa Cruz, 1156 High Street, Santa Cruz, CA 95064, USA

[2] Department of Molecular, Cell, and Developmental Biology, University of California Santa Cruz, 1156 High Street, Santa Cruz, CA 95064, USA

[3] Harvard Medical School, Blavatnik Institute, Department of Neurobiology, Boston, MA 02115, USA

[4] Stanley Center for Psychiatric Research, Broad Institute of MIT and Harvard, Cambridge, MA 02142, USA

[5] Department of Basic Medical Sciences, University of Arizona College of Medicine - Phoenix, Phoenix, AZ 85004, USA.

[6]Lead Contact

[#]Correspondence: bchen@ucsc.edu

[*] These authors contributed equally

Chapter 1: The cerebral cortex

Introduction

The human brain is the result of millions of years of evolution and is the source of our advanced processing power. Specifically, the neocortex is the biological substrate of our unique mental capabilities. These capabilities depend on a vast number of different cell types arranged in highly complex networks. Generally, these cell types are classified as neurons, cells specialized for electrical signaling and the primary informational units, and glia, the supporting cells. The human cortex contains approximately 16 billion neurons, a similar number of non-neuronal cells, and accounts for 82% of brain mass (Azevedo et al., 2009). The study of brain cells dates back over a century to Santiago Ramon y Cajal, and Camillo Golgi. Together, they pioneered the field of neuroanatomy and were awarded the Nobel Prize in 1906 in recognition of their work on the structure of the nervous system ("The Nobel Prize in Physiology or Medicine 1906," n.d.). Despite over one hundred years of progress, mechanisms behind the generation and differentiation of these neuronal and non-neuronal cells remains an important area of study.

Brain development in mammals begins in late gastrulation with the formation of the neural plate in a process called neurulation. The neural plate then folds inwards on itself to form the neural tube which will eventually give rise to the entire brain, spinal cord, and most of the peripheral nervous system. The neural tube consists of neuronal stem cells which divide and proliferate to produce regionalized primitive brain regions that undergo further partitioning to form five major subdivisions: telencephalon, diencephalon, mesencephalon, metencephalon, and myelencephalon. This thesis will focus on the telencephalic region known as the cerebral cortex. For more detailed information on early brain development and segmentation, see reviews: (*Neuroscience, 5th ed.*, 2012; Stiles and Jernigan, 2010).

The telencephalon is the largest part of the human brain and consists of the cerebral cortex, axonal projection fiber tracts, and basal nuclei. Primitive cortical structures first appear

in small mammals shortly after the Triassic period and have increased in size and complexity ever since (Rakic, 2009). Today, the fundamental architecture of the cortex of most mammals follows similar principles of organization. The “radial unit hypothesis” was first postulated by Rakic in 1988 and is still the accepted model for cerebral cortical formation. According to this hypothesis, the ependymal layer of the newly formed ventricle contains proliferative units that expand into columns creating a map of cytoarchitectural areas (Rakic, 1988, p. 19). This supports the notion that cortical expansion in evolution is mainly driven by an increase in cortical surface area rather than cortical thickness. For example, between mouse, macaque, and human cortices, there is a large increase in surface area 1:100:1000 x, respectively, and a relatively small change in thickness.

The cerebral cortex contains two main classes of cells, neurons and non-neurons, that are organized into a six layered laminar structure. Cortical projection neurons are the principle excitatory cells that underly cortical computation and primarily use glutamate as their neurotransmitter. Gamma-aminobutyric acid inhibitory neurons (GABAergic neurons) function to modulate excitation and signal transduction of the excitatory neurons and constitute about 20% of the neurons in the cortex (Sahara et al., 2012). Non-neuronal cells consist of several glial subtypes including, astrocytes, oligodendrocytes, and microglia, and serve many supportive roles to the projection neurons such as synapse support, axonal conduction support, and immune support, respectively (Allen and Lyons, 2018).

Cortical projection neurons can be classified several ways: spatially, transcriptionally, morphologically, electrophysiologically, hodologically, epigenetically, and molecularly, to name a few. Classically, cortical projection neurons have been classified in the following three categories according to location and hodology: corticothalamic projection neurons (CTPNs), subcerebral projection neurons (SCPNs), and intratelencephalic (IT) neurons. CTPNs mainly reside in layer 6 and project to the thalamus, SCPNs reside in layer 5 and project to the brainstem and spinal cord, and IT neurons are found throughout all layers, and project within

the cortex either locally (ipsilaterally), or to the opposite hemisphere (contralaterally) (Molyneaux et al., 2007).

A large effort in recent years has been made to systematically identify and classify the different cell types in the cortex with varying results. For example, characterization of cortical areas by single-cell RNA sequencing revealed as many as 133 distinct subtypes while characterization by MERFISH resulted in only 95 (Tasic et al., 2018; X. Zhang et al., 2020). Another group was able to categorize projection neurons into 11 distinct types based on morphology alone (Peng et al., 2021). Yet another study identified 15 epigenetically distinct clusters solely in layer 5 (Zhang et al., 2021). It has become apparent that one single method of categorization will not be sufficient and the most effective indexing will involve several methods. Nevertheless, understanding discrete differences in the vast diversity of cells in a mature cortex remains an important area of study.

Despite evolutionarily branching off from humans 100 million years ago, the mouse remains the favorite model system for human brain development. Short gestation times, inbred strains with consistent background genetics, multiple tools for genetic manipulation, and large litter sizes make the mouse a practical system. Biologically, the mouse cortex and human cortex have several similarities. Both contain a 6 layered laminar architecture with similar cell types, projections, functions, and organization of distinct regions. Cortical development of both organisms also follows a very similar chronology with radial glial cells (RGCs) serving as the principle proliferative units which undergo a series of divisions and migrations to form the cortical plate in an inside-out manner. Additionally, many of the intrinsic and extrinsic signals and transcription factors involved in this timing are highly conserved. For these reasons, I utilize the mouse as a model organism for studying mechanisms involved in cortical development and disease and will be referring to mouse cortex development for the remainder of this thesis unless otherwise noted.

Neural induction and initial patterning

Following the formation of the neural tube, the neural stem cells must receive instructions for their initial patterning. These instructions can come from cell-intrinsic or cell-extrinsic sources. The extrinsic signals are secreted ligands from neighboring tissue. The type of ligand received, as well as concentration gradient (dependent on the distance of target cells from the source), help direct the nascent stem cell towards its neural cell fate. Cell-intrinsic signals include expression of specific neural induction genes and changes in cell cycle length (Takahashi et al., 1995). The specific combination of these neural induction signals results in distinct signatures of gene expression that direct cell proliferation and establish different brain regions.

For example, initial neocortex patterning into the motor cortex (M1), somatosensory cortex (S1), and visual cortex (V1), depends on opposing expression gradients of signaling molecules Pax6, Emx2, SP8, and Coup-TF1. Pax6 expression is highest in the anterior-lateral regions while Emx2 expression is highest in the posterior-medial regions (Cadwell et al., 2019). Similarly, Coup-TF1 expression is highest in the caudal-lateral regions while Sp8 expression is highest in the rostral-medial regions. This set of opposing gradients create unique environments of signaling molecules across the landscape of the neocortical proliferative zone. When the expression of each of these genes is systematically blocked, cortical patterning is altered in a predicted manner (Hamasaki et al., 2004). This demonstrates the importance and intricacies of signaling molecules in the developing cortex.

Cortical plate formation

The developing cortical plate contains several distinct regions such as the ventricular zone (VZ), subventricular zone (SVZ), subplate (SP), cortical plate (CP), and preplate (PP). RGCs occupy the VZ, establish the apical/basal directionality, and provide the initial scaffolding for neuronal migration. RGCs are the result of neural inductive signals on the progenitor population from the neural tube. Named for their glial morphology, these are the multipotent

stem cells of the cortex. Every projection neuron and glial cell arises from this population of progenitors. They must undergo a vast number of divisions to account for the 16 billion neurons in the cortex. Initially, RGCs expand their population in the VZ through symmetric divisions before they begin to divide asymmetrically. These asymmetric divisions primarily result in another RGC and a Tbr2+ intermediate progenitor cell (IPC) but can also generate an immature neuron. These IPCs then divide symmetrically into two post-mitotic neurons. In this manner, they function as transit-amplifying cells and generate up to 80% of the excitatory projection neurons throughout all cortical layers (Kowalczyk et al., 2009; Taverna et al., 2014).

As more neurons are generated, they migrate into the cortical plate using the basal process of the parent RGC as a scaffold. Once they reach the correct position, they detach and integrate themselves laterally into a specific layer in the cortical plate. The earliest born neurons generate in the deepest (apical) layers while later born neurons migrate past the older born neurons and deposit themselves in the more superficial (basal) layers (Kwan et al., 2012; Leone et al., 2008). Therefore, the cortex is said to develop inside-out (Figure 1).

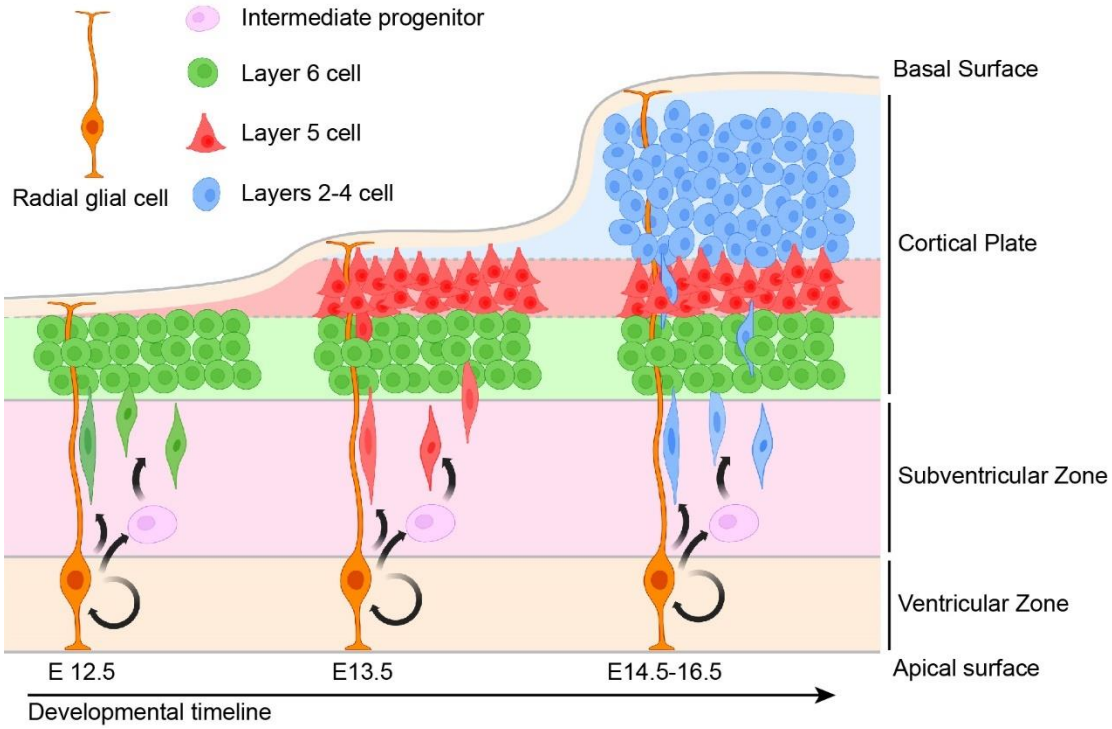

Figure 1: Developmental timeline diagram of the mouse cerebral cortex

As this process continues, the lineage potential of the RGCs is restricted. A seminal study by Susan McConnell in 1988 demonstrated that the early cortical progenitors are multipotent and can generate neurons in all cortical layers, but as developmental time progresses, these progenitors progressively lose their ability to generate the earlier temporal fates (McConnell, 1988). Since then, several studies have confirmed this hypothesis and the progressive fate restriction of RGCs in the developing cortex is now widely accepted. Furthermore, several studies have shown there are no unique fate-restricted RGCs that only generate a single cell type (all are multipotent), and neuronal specification occurs post-mitotically (Di Bella et al., 2021; Eckler et al., 2015; Gao et al., 2014; Guo et al., 2013).

Fate specification of excitatory projection neurons

The temporal process of RGC differentiation and laminar specification is tightly regulated and dependent on many factors. It has become clear that transcriptional regulation plays a central role in specifying the vast number of cell fates in the developing cortex. Indeed, several genes have been identified that are responsible for the specification of distinct classes of projection neurons. Many of these genes transcribe transcription factors with very specific spatial and temporal expression patterns. Several of these transcription factors function through successive repression to further restrict cell fate (Galazo et al., 2022; Han et al., 2011; Kwan et al., 2008; McKenna et al., 2015; Srinivasan et al., 2012; Tsyporin et al., 2021). For example, Satb2 is required for the specification of IT projection neurons. Satb2 recruits the NURD complex to the *Ctip2* promotor, directly repressing the expression of Ctip2. Congruent with this, in the absence of Satb2 expression, the IT neurons lose their upper layer identity and ectopically express subcerebral marker, Ctip2, and assume subcerebral phenotypes (Britanova et al., 2008a). Additionally, we recently showed that Fezf2 functions as a transcriptional repressor, through recruitment of Tle4, in subcerebral neurons. Only a chimeric protein of Fezf2 and a strong repressor was able to rescue the Fezf2 KO phenotype. The chimeric protein of Fezf2 and an activator domain had no effect (Tsyporin et al., 2021). A graphical summary of examples of laminar specification is presented in Figure 2.

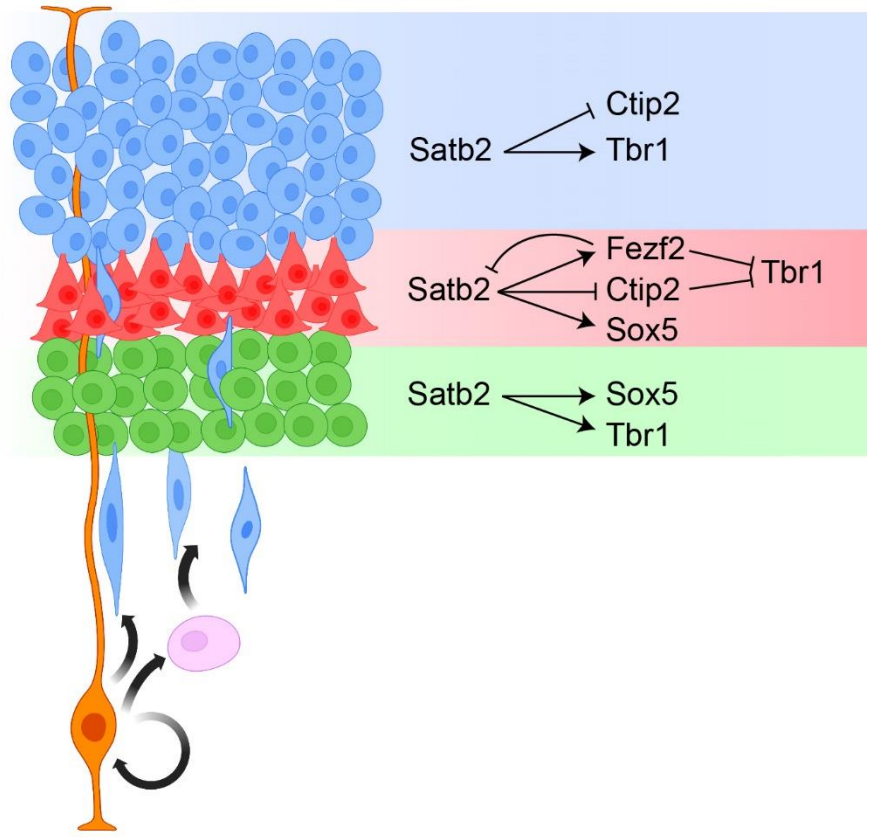

Figure 2: Example of the repression and activation network of transcription factors during fate specification

Generation of glial cells

At the end of cortical neurogenesis, around embryonic day 16 (E16) in the mouse, RGCs switch to generating cortical glial cells. Upon Sonic hedgehog (SHH) signaling, the RGCs begin to generate Gxs2+ IPCs, instead of Tbr2+ IPCs. These Gsx2+ IPCs are tripotent and give rise to olfactory bulb interneurons, cortical oligodendrocytes, and cortical astrocytes (Y. Zhang et al., 2020). Similar to the projection neurons, astrocytes utilize RGC processes to guide their migration into the cortical plate (Burns et al., 2009). Oligodendrocyte precursors, however, use the scaffold of blood vessels to guide their migration, detaching once they reach

astrocyte end-foots (Su et al., 2023). At the end of gliogenesis, RGCs undergo final symmetric divisions to generate the last IPCs, concluding the lifecycle of the radial glial cell.

Conclusions

This chapter is a brief overview on mammalian cortical development. Its purpose is to highlight the complexity of the cortex and lay the foundation for the remainder of this thesis. The focus of my thesis work is to elucidate discrete mechanisms involved in this process and provide insight into what goes wrong in human diseases associated with mutations in these transcription factors. Chapter 2 will introduce Satb2, the main character of my work, and its role in development and disease.

Chapter 2: Satb2 in development and disease

Overview

Special AT-rich Sequence DNA binding protein 2 (SATB2) was first identified in 2003 as a cleft palate gene and a nuclear matrix attachment region (MAR) binding protein (Dobreva et al., 2003, p. 20; FitzPatrick, 2003; Kikuno, 2002). Since then, it has been implicated in numerous important biological pathways in a variety of organs, systems, and species. Briefly, Satb2 plays a role in osteoblastogenesis and skeletal development by directly regulating expression of transcription factors (TFs) that regulate osteoblast differentiation (Dobreva et al., 2006a; Zhang et al., 2011). Accordingly, it is also responsible for facial patterning, jaw development, and even promotes differentiation of hIPSCs toward an osteoblast lineage (Britanova et al., 2006; Dobreva et al., 2006a; Fish et al., 2011; Ye et al., 2011). Due to the activity of Satb2 as a chromatin organizer, and the fact that abnormal regulation of chromatin structure occurs in most cancer cells, it has also been implicated in glioblastomas, breast cancer, and tumor progression (He et al., 2008; Luo et al., 2016; Naik and Galande, 2019; Patani et al., 2009; Tao et al., 2020). Satb2 even plays a role in electrosensory ampullary organ development in electroreceptive jawed vertebrates (Minařík et al., 2023).

All of these functions aside, this thesis focuses on the critical role Satb2 plays in cortical development and, when mutated, developmental diseases. The cortex specific functions of Satb2 are reviewed below.

Satb2 structure, conservation, and tissue expression

The *SATB2* gene in humans is located on the long arm of chromosome 2, is around 200 kb in size, and contains 10 introns and 11 exons. The transcription start site is located in exon 2 and the open reading frame spans through exon 11. *Satb2* transcription is temporal and lineage specific and is regulated by a variety of growth factors, receptor pathways, and micro-

RNAs (Bonilla-Claudio et al., 2012; Dobreva et al., 2003; Jiang et al., 2015; Luo et al., 2016; Tang et al., 2011).

Satb2 encodes a protein consisting of 733 amino acids, containing five functional domains: one ubiquitin like domain (ULD), one cut repeat like domain (CUTL), two cut domains (CUT1 and CUT2), and a homeobox domain (HOX). Satb2 is a member of the Satb family of proteins and is closely related to Satb1 (Britanova et al., 2005; Lozano et al., 2023; Naik and Galande, 2019; Szemes et al., 2006). Satb1 was identified over a decade before Satb2, and as such, the majority of structural analysis has been performed on Satb1 (Dickinson, 1992). Due to the high sequence homology in the functional domains, we can assume the Satb2 domains function in similar manners.

The ULD, previously identified as a PDZ domain, is located on the N-terminal region of Satb2 and is responsible for self-oligomerization and interactions with other proteins (Galande et al., 2001; Gyorgy et al., 2008; Kumar et al., 2005, p. 202; Wang et al., 2012). It is unclear whether Satb1 and Satb2 can form heteromers or if they are only able to function as homomers. Oligomerization is required for Satb1/2 to bind the DNA in a sequence specific manner (Galande et al., 2001; Purbey et al., 2008; Wang et al., 2012). The Satb1 tetramer was shown to be able to bind two DNA targets simultaneously by isothermal titration calorimetry (Wang et al., 2012). In addition to self-oligomerization, the ULD has also been implicated in interactions with other proteins. Immunohistochemistry and chromatin immunoprecipitation experiments have shown Satb2 co-expressing and interacting with NURD proteins Hdac1 and Mta2 (Britanova et al., 2008a; Gyorgy et al., 2008).

The two CUT domains are DNA binding motifs that confer sequence specific DNA binding to Satb2. Specifically, these domains recognize core unwinding elements in MAR domains and enhance interactions in the major groove of the DNA (Dickinson et al., 1997; Nakagomi et al., 1994; Purbey et al., 2008; Yamasaki et al., 2007).

Similarly, the CUTL domain also has DNA binding activity. A study that utilized a ULD-CUTL tandem domain determined that the ability of Satb21 to bind DNA depends on the CUTL

domain. Additionally, the CUTL domain was shown to be essential for DNA binding of full length Satb1 (Wang et al., 2014).

Lastly the HOX domain was shown to not strongly bind DNA by itself, but functions to enhance the binding specificity of the core unwinding element of a MAR (Dickinson et al., 1997).

The function of Satb2 cannot be traced back to a single domain. It is clear that all domains work together to enhance binding activity and specificity to MARs in the genome. Further work needs to be done to determine if the subunit composition of the Satb oligomer plays a role in the overall activity or specificity.

Satb2 has striking conservation across many species (Sheehan-Rooney et al., 2010). Compared to the human SATB2 amino acid sequence, both the Chimpanzee and Bonobo have 100% sequence homology. Man's best friend, the Canine, Alpacas, and mice all share 99% homology with humans. Unfortunately, most research labs are too small to efficiently house Alpacas, so most research is performed with mice. In fact, the human SATB2 and Mouse Satb2 proteins only differ by 3 AA out of 733. I481V is in the CUT2 domain while both A590T and I730T are located in disordered regions. This homology, in addition to reasons discussed in Chapter 1, makes the mouse an ideal organism to study the function of Satb2 in cortex development.

In humans, SATB2 is expressed in several tissues. The highest expression occurs in the gastrointestinal tract, bone marrow and lymphoids, and brain tissue ("Tissue expression of SATB2 - Summary - The Human Protein Atlas," n.d.). Within the brain, SATB2 expression is mainly restricted to the cortex, hippocampus, and basal ganglia. This tissue expression profile is also seen in the mouse.

Role of Satb2 in cortex development

Satb2 is expressed in all layers of the cortex and is primarily expressed in excitatory projection neurons. Immunostaining showed all Satb2+ cells co-stain with neuronal marker,

NeuN, with no overlap of glial markers S100 or GFAP (Huang et al., 2013). Like other transcription factors, Satb2 is not expressed in proliferating cells in the dorsal telencephalon (Britanova et al., 2005; Szemes et al., 2006). Its expression can be detected as early as E13.5 but shows a “post-mitotic waiting period” for the first nine hours after mitotic cycle exit before expression can be detected. 24 hours after mitotic cell exit, strong labeling can be seen in neurons (Britanova et al., 2008a). This supports the notion that cortical fate specification occurs post-mitotically as discussed in Chapter 1.

Although most transcription factors in the cortex function through repression of target genes, Satb2 can both repress and activate its targets in a cell type dependent manner. For example, in upper layers 2/3, Satb2 directly represses *Ctip2* transcription through Ski mediated recruitment of Hdac1. In the absence of Satb2, these neurons ectopically express Ctip2 and fail to extend their axons through the corpus callosum. By repressing *Ctip2*, Satb2 blocks these neurons from acquiring SCPN properties and instead directs them toward a callosal neuron identity (Alcamo et al., 2008; Baranek et al., 2012; Britanova et al., 2008a). However, in layer 5, Satb2 directly promotes transcription of *Fezf2* and *Sox5* to promote subcerebral identity. This high level of Fezf2 then represses *Satb2* expression, preventing Satb2 from activating any callosal genes and allowing other subcerebral genes to be expressed, such as *Ctip2* (McKenna et al., 2015; Srinivasan et al., 2012). In layer 6, Satb2 instead promotes *Sox5* and *Tbr1* expression imparting subcerebral or corticothalamic identity (Srinivasan et al., 2012). In layer 4, Satb2 promotes *Rorb* expression which is required for barrel integrity, expression of layer 4 genes, repression of layer 5 genes, and thalamocortical afferent organization (Alcamo et al., 2008; Clark et al., 2020, p. 20).

In addition to specifying laminar organization of cell types, Satb2 is also responsible for specification of axonal projections. Due to unrestricted expression of *Satb2* in the upper layers, it is normally referred to as a callosal neuron identifier. Indeed, Satb2 is highly expressed in these IT neurons that project both ipsi- and contralaterally. In the absence of Satb2, normal axon guidance through the corpus callosum is missing. Instead, there is an

increase in subcerebral projections and axons crossing the anterior commissure (Alcamo et al., 2008; Britanova et al., 2008b; Leone et al., 2015a, p. 201). Interestingly, the increase in subcerebral projections does not arise from misguided upper layer axons but from misguided layer 5 Rbp4+ neuronal projections (Leone et al., 2015a). Further, these axons were still present when *Satb2* was knocked out in layer 5, after the establishment of layer 5 neurons, with Rbp4-cre. This suggests that Satb2 plays an early role in the specification of neuronal projections, prior to E17.5 when Rbp4-cre is expressed (Leone et al., 2015a).

Several genes involved in establishing projections of callosal neurons are directly controlled by Satb2. Netrin1 receptors DCC and Unc5c are directly repressed and promoted by Satb2, respectively (Srivatsa et al., 2014). Both DCC and Unc5c have been shown to be key regulators in the guidance of commissural axons in vertebrate development and have opposing functions (Keino-Masu et al., 1996; Kennedy et al., 1994; Kim and Ackerman, 2011). DCC imparts an attractive response to Netrin 1 signaling while Unc5c imparts a repulsive response. In *Satb2* homozygous mutants, there is a large increase in DCC expression and a decrease in Unc5c and callosal projection neurons are misguided. Accordingly, these misguided callosal axons in Satb2 homozygous mutants can be partially rescued with downregulating DCC or overexpressing Unc5c (Srivatsa et al., 2014).

Other misregulated Satb2 dependent genes have been shown effective at rescuing callosal axons as well. The axonal guidance molecule, EphA4, is downregulated in the upper layers of *Satb2* homozygous mutant mice. In utero electroporation of *EphA4* was shown to rescue the extension of axons across the corpus callosum of mutant mice, confirming it functions downstream of *Satb2* in callosal fate specification. Interestingly, overexpression of Tbr1 in the upper layers of *Satb2* homozygous mutant cortices is also effective at rescuing callosal identity. As well as promoting Tbr1 expression in deep layers, Satb2 promotes Tbr1 expression in the upper layers where it aids in establishing callosal identity (Srinivasan et al., 2012).

Satb2 plays critical roles in all cortical layers for fate specification and projection guidance. Few, if any, transcription factors have this breadth of effect. For this reason, Satb2 is often referred to as a “master regulator” in cortical development. Due to its wide-ranging functions, mutations associated with *Satb2* have severe consequences, as reviewed below.

SATB2-Associated Syndrome

SATB2-Associated Syndrome (SAS, OMIM #612313) is caused by heterozygous *de novo* mutations in *SATB2*. Deletions on the distal region of chromosome 2 have been described for over 40 years with consistent phenotypes (Sills et al., 1976). It wasn’t until 2003 that *SATB2* was associated with cleft palate, 2007 when the first specific heterozygous nonsense mutation was found in *SATB2*, and 2014 when SATB2-Associated Syndrome was proposed as a clinically recognized syndrome (Döcker et al., 2014; FitzPatrick, 2003; Leoyklang et al., 2007). At the time of this thesis, 750 patients with SATB2-Associated Syndrome have been diagnosed across 50 countries with over 100 unique gene variants (“satb2gene.org,” n.d.; Zarate et al., 2019).

Genetic alterations in SAS patients include large chromosomal deletions encompassing *SATB2*, nonsense and missense single nucleotide variants, intragenic deletions and duplications, and splice-site alterations (Bengani et al., 2017). Approximately 70% of these alterations are likely loss-of-function mutations, while the other 30% have unknown effects on SATB2 function. Clinical symptoms associated with SAS are often co-occurring and debilitating. Two main symptoms seen in the majority of patients are severe intellectual disability and delayed or absent speech. In addition to these, patients can present with a variety of other symptoms and combinations of symptoms including: seizures, palatal and dental anomalies, dysmorphic facial features, microcephaly, lissencephaly, behavioral problems, and feeding difficulties (Bissell et al., 2022; Döcker et al., 2014; Kikuiri et al., 2018; Leoyklang et al., 2007; Lewis et al., 2020; Lo et al., 2022; Zarate et al., 2019; Zhao et al., 2014).

Conclusions

Despite decades of research, there are no cures or therapeutic options and research into *Satb2* haploinsufficiency has been scarce. Moreover, several studies use Satb2 heterozygotes interchangeably with wildtype mice in the search for Satb2 function. Although these studies have identified major roles for Satb2 in cortical development, focused research on the effects of *Satb2* haploinsufficiency, development and characterization of a mouse model, and potential therapeutic options need to be explored. The focus of the research in this dissertation is creating and characterizing a mouse model for heterozygous loss-of-function, as seen in SAS, identifying the dose dependent effects of Satb2 in cortical development, and elucidating mechanisms involved in the disease.

Chapter 3: *Satb2* haploinsufficiency results in altered chromatin landscape, aberrant IT neuronal projections, and human disease

Summary

Heterozygous *de novo* mutations in Special AT-rich Sequence Binding Protein 2 (SATB2) result in SATB2-Associated Syndrome (SAS), a recently described human disease characterized by developmental defects and intellectual deficiency. SATB2 expression in the brain is mostly restricted to the excitatory neurons in the cerebral cortex and the hippocampus, suggesting that the intellectual deficiency associated with SAS is likely due to defective cortical and hippocampal neurons. Extensive studies show that Satb2 regulates gene expression and plays a crucial role in specifying the identities of multiple cortical projection neuron subtypes. However, these studies were performed using *Satb2* homozygous mutant mice. It remained unknown how *SATB2* heterozygous loss-of-function mutations, as commonly seen in SAS patients, affects brain development. Utilizing *Satb2* heterozygous deficient mice, we show that *Satb2* haploinsufficiency leads to gene mis-regulation, physiological changes, aberrant axonal projections, and cortical lamination defects. Chromatin immunoprecipitation and CUT&RUN experiments reveal that Satb2 binds to gene promoters and enhancers. We show that Satb2 both activates and represses gene expression, by recruiting distinct chromatin remodeling complexes. Our findings uncover fundamental mechanisms underlying cortical projection neuron development and the etiology of SAS.

Introduction

The 6-layered neocortex is the seat of the most complex cognitive and perceptual functions in humans. Glutamatergic projection neurons occupy a central position in cortical neural circuits, serving as the principal input units and the sole output system. Although single-cell RNA-seq analysis has revealed many refined subtypes (Tasic et al., 2018; Zeng, 2022), cortical excitatory neurons can be broadly classified into three major subtypes based on

hodology: corticothalamic (CT) neurons in layer 6 that project to the thalamus, subcerebral projection neurons (SCPNs) in layer 5b that projection to the midbrain, hindbrain, and spinal cord, and intratelencephalic (IT) neurons that reside throughout layers 2-6 and project to the ipsi- or contra-lateral cortical hemisphere (Greig et al., 2013a; Leone et al., 2008).

During development, cortical excitatory neurons arise directly from radial glial cells (RGCs) or indirectly from intermediate progenitors (Kriegstein and Alvarez-Buylla, 2009; Malatesta et al., 2000; Miyata et al., 2001; Noctor et al., 2001). The earliest-born neurons form the preplate which is split into the marginal zone and subplate by incoming cortical plate neurons. The excitatory neurons within the cortical plate arise in a temporal sequence where layer 6 neurons are produced first, followed by increasingly superficial layers up to layer 2 (Leone et al., 2008). Proper generation and differentiation of the cortical excitatory neurons is essential for normal cortical functions.

Extensive progress has been made toward delineating the molecular mechanisms underlying the production of distinct excitatory neuron subtypes. Development of distinct projection neuron subtypes depends on a network of transcription factors that mostly cross-inhibit the expression of one another (Greig et al., 2013b). The zinc-finger transcription factor Fezf2 is expressed in deep-layer neurons where it promotes subcerebral neuronal identity while suppressing the expression of cell fate determining genes for corticothalamic (*Tbr1*) and callosal (*Satb2*) neurons (B. Chen et al., 2005; Chen et al., 2008a; J.-G. Chen et al., 2005; Molyneaux et al., 2005; Tsyporin et al., 2021). Tbr1 and Sox5 promote corticothalamic neuronal fate and directly repress high levels of Fezf2, and thus subcerebral identity, in layer 6 neurons (Han et al., 2011; Kwan et al., 2008; Lai et al., 2008; McKenna et al., 2011). Satb2 was reported to be specifically expressed in callosal neurons and promote callosal neuron identity by repressing essential genes for subcerebral axon development (Alcamo et al., 2008; Britanova et al., 2008a). Further studies revealed that Satb2 is also required for specifying layer 5 subcerebral neuron identity (McKenna et al., 2015).

SATB2-Associated Syndrome (SAS) is a newly identified neurodevelopmental disease that is characterized by developmental delay, severe intellectual deficiency with absent or limited speech, behavioral problems, and dysmorphic craniofacial features (Zarate et al., 2017). It is caused by heterozygous *de novo* mutations of *SATB2*, a DNA-binding protein involved in chromatin remodeling, often leading to loss-of-function. In the brain, *SATB2* expression is mainly restricted to the projection neurons in the cerebral cortex and hippocampus, suggesting that the etiology of the intellectual deficiency of SAS is likely defective cortical and hippocampal projection neurons.

Studies in mice have shown that Satb2 is required for specifying the subtype identities of both cortical callosal and SC neurons. In *Satb2* homozygous mutant mice, callosal neurons lose their molecular and axon projection identities, and express genes associated with layer 5 SC neurons, while the layer 5 SC neurons are missing and fail to extend axons to the brainstem and spinal cord (Alcamo et al., 2008; Britanova et al., 2008a; Leone et al., 2015b; McKenna et al., 2015). By recruiting the nucleosome remodeling deacetylase (NuRD) complex, Satb2 represses the expression of *Bcl11b,* a gene essential for axonal projections of layer 5 SC neurons (Alcamo et al., 2008; Britanova et al., 2008a). Despite these discoveries, the underlying molecular logic for how Satb2 broadly regulates gene expression programs is unknown. Furthermore, prior studies on Satb2 function in brain development were performed using homozygous mutant mice (Alcamo et al., 2008; Britanova et al., 2008a; Leone et al., 2015b; McKenna et al., 2015). It remains to be determined how heterozygous loss-of-function of *SATB2*, as identified in SAS patients, affects brain development.

Here, using Satb2 heterozygous deficient mice, we demonstrate that Satb2 is responsible for proper cortical laminar organization, intra-telencephalic axon development and gene expression in a gene-dosage-dependent manner. Our CUT&RUN analysis revealed that Satb2 directly regulates numerous genes implicated in cell fate specification as well as genes critical for cell adhesion, axon guidance, and neuronal physiology. We find that Satb2-mediated gene activation and repression is likely facilitated by the interaction of Satb2 with ATP-

dependent chromatin remodeling complexes. Furthermore, we show that proper Satb2 dosage is required for cortical layer formation and that *Satb2* haploinsufficiency affects IT neuron axon projections, gene expression programs, and neuronal physiology while sparing the SCPN and CT neuron projections, providing insights into the molecular underpinning of SAS etiology.

Results

Satb2 haploinsufficiency leads to defective cortical laminar organization

To examine how *SATB2* haploinsufficiency affects brain development, we utilized *Satb2*$^{lacZ/+}$ mice, which carry a beta-galactosidase gene inserted at the start of the *Satb2* open reading frame (*Satb2*^{lacZ}) (Dobreva et al., 2006b), effectively knocking out the *Satb2* gene (Figure 4B). Western blot analysis revealed a 50% decrease of Satb2 protein in P0 *Satb2*$^{lacZ/+}$ cortices and absence of Satb2 protein in P0 *Satb2*$^{lacZ/lacZ}$ cortices (Figure 3A).

We analyzed *Satb2*$^{+/+}$ and *Satb2*$^{lacZ/+}$ brains collected at postnatal day 1 (P1), P4, P7, and P28 (Figure 3B-3E). Immunostaining for markers of different cortical projection neuron subtypes and nuclear staining did not show any significant change in the *Satb2*$^{lacZ/+}$ cortices at P1 (Figure 3B and 3D). Comparing cortices from *Satb2*$^{+/+}$ *and Satb2*$^{lacZ/+}$ mice at P4, P7, and P28 revealed changes in the thickness of cortical layers (Figure 3B-3E).

At P28 *Satb2*$^{lacZ/+}$ mice showed a 23.2% reduction for layer 6 (*Satb2*$^{+/+}$: 333.0 ± 22.5 µm (SEM) vs. *Satb2*$^{lacZ/+}$: 255.7 ± 15.6 µm), 38.6% reduction for layer 4 (*Satb2*$^{+/+}$: 133.1 ± 6.0 µm vs. *Satb2*$^{lacZ/+}$: 81.8 ± 2.9 µm), and 13.7% increase for layer 1 (*Satb2*$^{+/+}$: 107.8 ± 12.8 µm vs. *Satb2*$^{lacZ/+}$: 123.6 ± 19.5 µm) in the S1 barrel field (BF) area, while the thickness for layer 5 and layers 2/3 was not significantly affected (Figure 3B-3E).

Layer 6 projection neurons include corticothalamic neurons (CT), intra-telencephalic neurons (IT), and a small population of deep-layer near-projecting neurons (DLNP) neurons, which can be distinguished by Tbr1 and Tle4 expression. L6 CTs and DLNPs express both Tbr1 and Tle4 (Tbr1^{+}Tle4^{+}), while L6 IT neurons express Tbr1 but not Tle4 (Tbr^{+}Tle4^{-}). The

Satb2$^{lacZ/+}$ cortices showed a significant reduction of Tbr1^{+} neurons in layer 6 of at P4, P7, and P28. Among the Tbr1^{+} neurons, the numbers of Tbr1^{+}Tle4^{-} L6ITs were significantly reduced, while the numbers of Tbr1^{+}Tle4^{+} CTs and DLNPs were not significantly affected (Figure 3B and 3E), suggesting that *Satb2* haploinsufficiency results in a significant loss of L6IT neurons.

We examined layers 2-4 using antibodies for Rorb, Cux1 and Lhx2. We found that in the *Satb2*$^{lacZ/+}$ brains, the number of Rorb^{+} cells in layer 4 was significantly decreased in S1BF but increased in the more medial S1 Trunk (Tr) region (Figure 5A). A similar change for Cux1 expression was also observed, indicating a patterning defect of the S1Tr and S1BF regions. Immunostaining did not reveal neuronal subtype marker changes in layer 5 of the *Satb2*$^{lacZ/+}$ cortices (Figure 5D).

To investigate the cause of the thinner layer 6 and reduced Tbr1+ L6 ITs in the *Satb2*$^{lacZ/+}$ cortices (Figure 3B and 3E), we examined the expression between Tbr1 and Satb2, and observed that Satb2 and Tbr1 were co-expressed as early as E13.5 and throughout embryogenesis. Thus, Satb2 is expressed in these neurons at or around the time of their birth (Figure 4C).

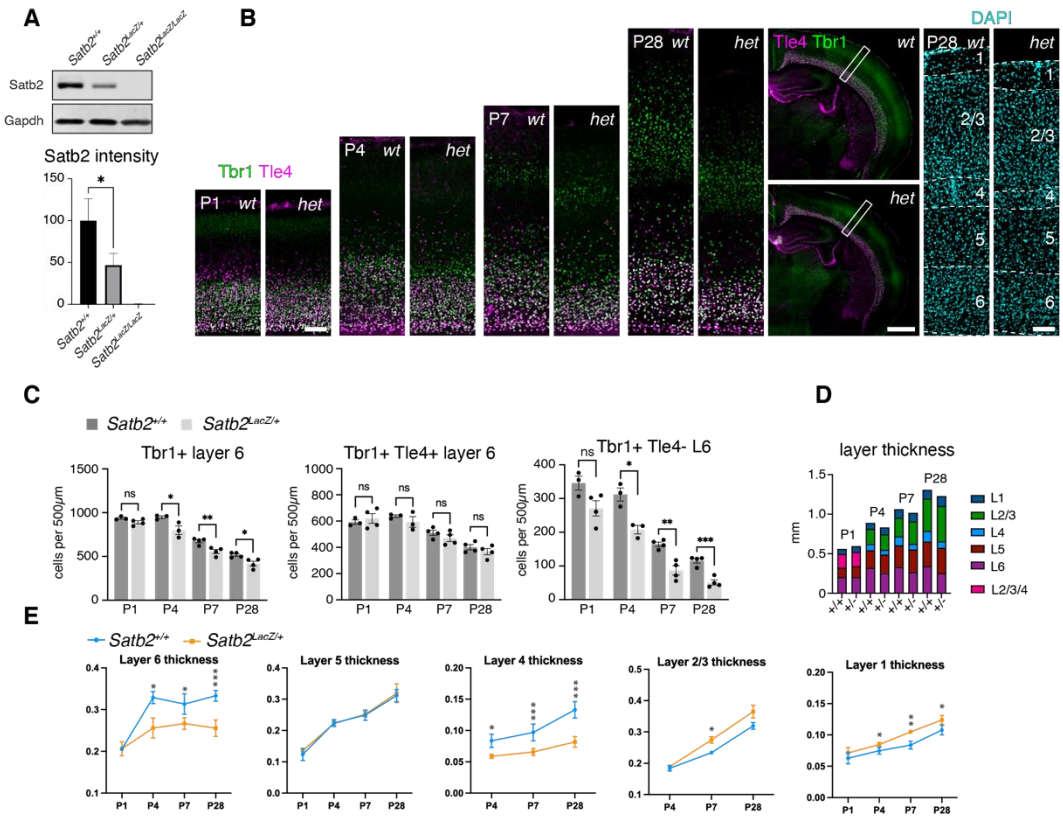

Figure 3: Layer size defects in *Satb2$^{lacZ/+}$* cortices

(A) Western blot showing a reduction and absence in *Satb2$^{LacZ/+}$* and *Satb2$^{LacZ/LacZ}$* cortices. Satb2 signal was normalized to Gapdh signal in each lane. n = 3 brains per genotype. Statistical significance was determined using student's t-test (* $p < 0.05$)
(B) Immunostaining for Tbr1 and Tle4 on brain sections from P1, P4, P7, and P28 *Satb2$^{+/+}$* and *Satb2$^{LacZ/+}$* mice, and DAPI at P28.
(C) Quantifications of marker^{+} cells per 500µm wide section in layer 6. n = 3-4 brains per genotype, 3-4 sections per brain.
(D) Quantification of layer thickness in mm
(E) Quantification of layer thickness split up by individual layers.
In all graphs, n = 3-4 brains per genotype, 3-4 sections per brain. Error bars represent ± SEM. Statistical significance was determined using nested t-test (*$p < 0.05$, **$p < 0.01$, ***$p < 0.001$)

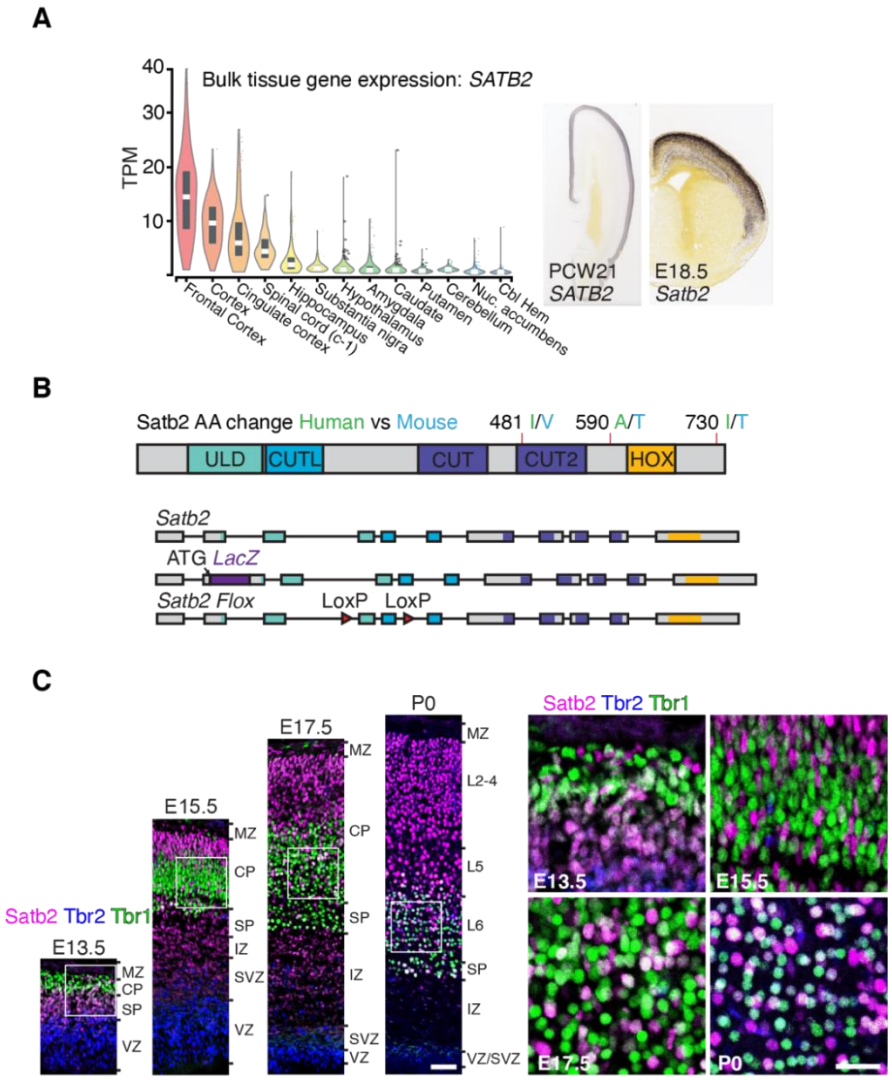

Figure 4: Satb2 is conserved between mouse and human and expressed across cortical layers

(A) Bulk tissue gene expression for *SATB2* and images from Allen Brain Atlas from PCW21 human embryo or E18.5 mouse embryo in-situ for *SATB2* or *Satb2* respectively.
(B) Diagram of Satb2 showing ammino acid changes between human and mouse. Blow is a diagram of the *Satb2* gene, $Satb2^{LacZ}$ allele, and $Satb2^{Flox}$ allele. ULD: ubiquitin-Like Domain, responsible for oligomerization. CUTL: CUT-like domain, similar to CUT domain, DNA binding motif. HOX: homeobox domain, DNA binding.
(C) Immunostaining for Satb2, Tbr2, and Tbr1 at E13.5, E15.5, E17.5, and P0. Satb2 expression is seen as early as E13.5 and co-expressed with Tbr1 but not Tbr2. Low mag scale bar 100µm, high mag scale bar 50µm.

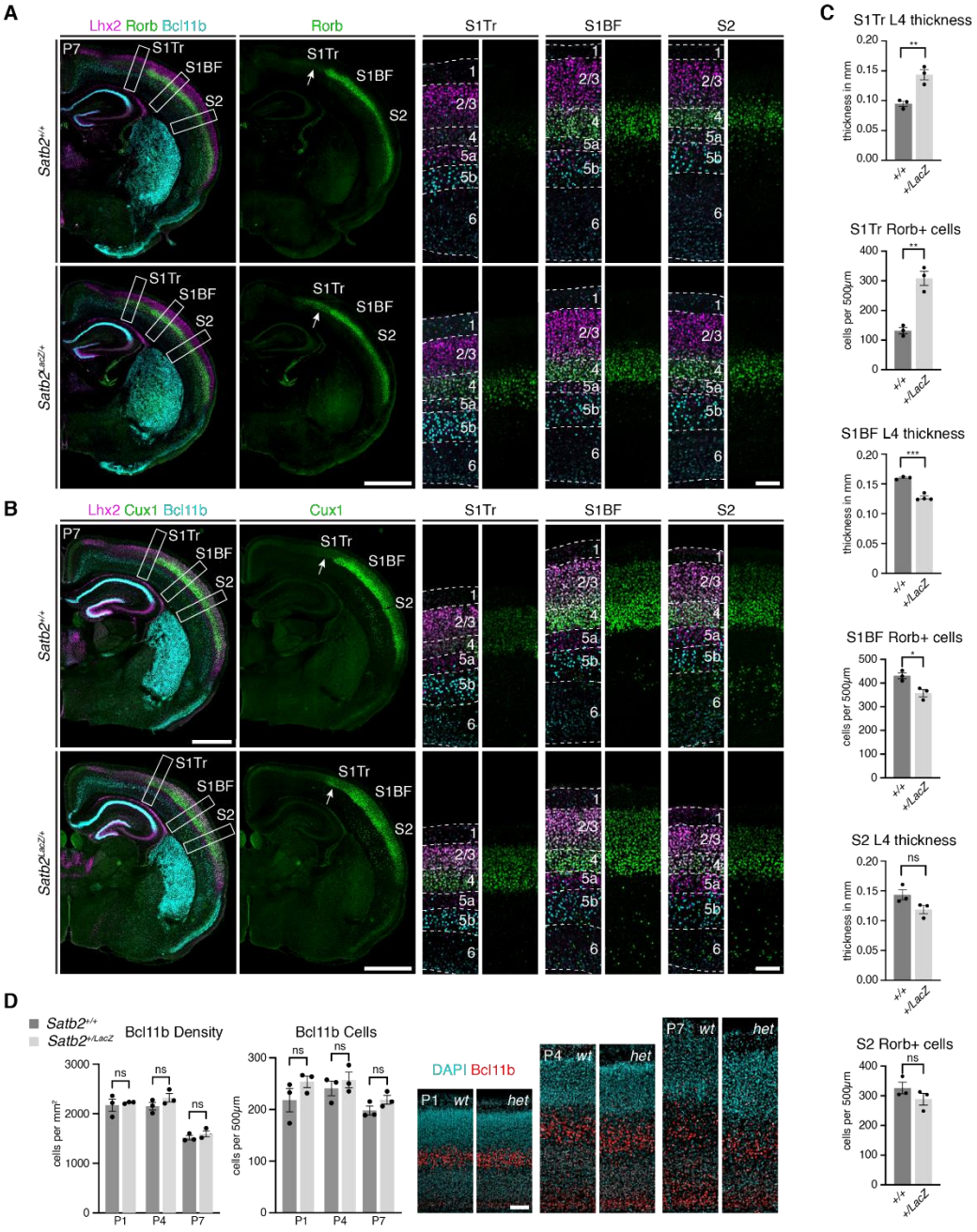
A
Lhx2 Rorb Bcl11b
Rorb
S1Tr
S1BF
S2
P7
Satb2+/+
Satb2LacZ/+
B
Lhx2 Cux1 Bcl11b
Cux1
C
S1Tr L4 thickness
thickness in mm
S1Tr Rorb+ cells
cells per 500μm
S1BF L4 thickness
S1BF Rorb+ cells
S2 L4 thickness
S2 Rorb+ cells
+/+
+/LacZ
D
Satb2+/+
Satb2+/LacZ
Bcl11b Density
cells per mm2
Bcl11b Cells
P1
P4
P7
ns
DAPI Bcl11b
wt
het

Figure 5: *Satb2*$^{LacZ/+}$ cortex exhibits thinner layer 4 in S1BF, and expansion of S1BF into S1Tr while layer 5 is unaffected

(A) Immunostaining for Lhx2, Rorb, and Bcl11b in P7 *Satb2*$^{+/+}$ and *Satb2*$^{LacZ/+}$ cortices. L2/3 and 5a marker Lhx2 and 5b marker Bcl1b are unaffected in *Satb2*$^{LacZ/+}$ cortices, while Rorb expression is decreased in L4 S1BF, expanded in S1Tr (white arrow), and unchanged in S2. Low magnification scale bar: 1000 µm, high magnification scale bar: 100 µm.
(B) Cux1 expression shows expansion into S1Tr (white arrow) in *Satb2*$^{LacZ/+}$ cortices. Low magnification scale bar: 1000 µm, high magnification scale bar: 100 µm.
(C and D) Quantifications of marker^{+} cells per 500 µm wide section. n = 3-4 brains per genotype, 3-4 sections per brain. Error bars represent ± SEM. Statistical significance was determined using nested t-test (*$p < 0.05$, **$p < 0.01$)

Satb2 haploinsufficiency results in defective callosal and thalamocortical projections

We examined whether *Satb2* haploinsufficiency impacts axon development. Immunostaining with L1 antibody revealed that in *Satb2*$^{LacZ/+}$ mice, the corpus callosum length was significantly reduced along the anterior-posterior axis at P7 (Figure 6A). (*Satb2*$^{+/+}$: 2601 ± 126 µm; *Satb2*$^{LacZ/+}$: 2043 ± 67 µm; n = 10 mice per genotype, p = 0.0010, unpaired t-test). L1 and PKCγ staining did not reveal significant changes in corticothalamic and corticospinal axons. Ntng1 is highly expressed in the thalamic neurons and labels the thalamocortical axons (TCAs). In the *Satb2*$^{LacZ/+}$ cortices, Ntng1 staining in layer 4 in S1 was reduced, indicating less cortical TCA innervation (Figure 6B). We examined barrel fields, an easily discernable target of TCAs, using cytochrome oxidase (CO) staining. Barrel organization was easily discernable in *Satb2*$^{+/+}$ cortices, however, in *Satb2*$^{LacZ/+}$ cortices, the barrel field was smaller overall, and the α row of barrels was consistently missing (Figure 6B).

To systematically examine the callosal, subcerebral, and corticothalamic projections, we injected Cholera toxin subunit B (CtB) into the corpus callosum (CC) close to the midline, cerebral peduncle (CP), and ventral posterior medial nucleus of the thalamus (VpM) at P28 and examined the brains at P33 (Figure 7). When CtB was injected into the CC, we observed both retrogradely labeled cells (and their axons) and anterogradely labeled axons in the *Satb2*$^{+/+}$ and *Satb2*$^{LacZ/+}$ mice (Figure 7A). We observed CtB-labeled cells and axons across layers 2/3, 5, and 6 in the ipsi- and contralateral cortex in controls. However, in *Satb2*$^{LacZ/+}$ cortices, there was a near absence of cells and axons labeled in layers 2/3 and reduced labeling of cells and axons in layers 5 and 6 in the somatosensory regions (Figure 7A). In the more medial region, the labeling in the medial parietal association (MPtA) region of the cortex was similar to the *Satb2*$^{+/+}$ mice (Figure 7A). Injection into the CP revealed no discernable difference in labeling the layer 5 SCPNs between *Satb2*$^{+/+}$ and *Satb2*$^{LacZ/+}$ cortices (Figure 7B): CtB labeled cells were abundant in layer 5b, and all labeled cells expressed the layer 5b SCPN marker Bcl11b but not Tbr1 (Figure 7B). Brains injected with CtB into the VpM showed all CtB-labeled cells co-expressed CT markers Tbr1 and Tle4 (Figure 7C). No difference in the number

of layer 6 CTs labeled between *Satb2*$^{+/+}$ and *Satb2*$^{LacZ/+}$ cortices. However, in the *Satb2*$^{LacZ/+}$ mice, the CtB+ cells were more densely packed, consistent with the distribution of Tbr1^{+}Tle4^{+} neurons in these cortices (Figure 7C). These findings reveal that *Satb2* haploinsufficiency leads to a severe reduction in callosal projection neurons located in somatosensory regions, while the number of callosal projection neurons more medially (MPtA region) were spared (Figure 7A).

Thus, *Satb2* haploinsufficiency differentially affects the major cortical axon pathways. The subcerebral and corticothalamic axon projections (Figure 7B and 7C) were mostly unaffected. However, there was almost complete absence of CtB^{+} callosal neurons and axons in layer 2/3, and severely reduced labeling of CtB^{+} callosal neurons and axons in layers 5/6 in S1 and S2 in the *Satb2*$^{LacZ/+}$ mice (Figure 7A). These results, combined with the results from the previous section, show that *Satb2* haploinsufficiency leads to broad defects in cortical ITs.

The reduction of Ntng1 signal in layer 4 of the *Satb2*$^{LacZ/+}$ brain suggested that Satb2 expression in the cortex may play a role in TCA innervation and targeting. To determine the requirement of Satb2 for TCA innervation of the cortex, we utilized a conditional *Satb2* expression allele, *Satb2*^{Flox}, and *Emx1*^{Cre} (Gorski et al., 2002) to generate *Satb2*$^{LacZ/flox}$; *Emx1*^{Cre} (*Satb2 cko*) mice. We previously validated that Satb2 expression is entirely absent in the *Satb2 cko* cortex (McKenna et al., 2015). In the *Satb2 cko*, we observed a complete lack of barrel fields visualized by Ntng1 and CO staining in the cortex, but there was still diffuse Ntng1 staining within the cortex and subplate, indicating that TCAs can cross the pallial-subpallial boundary and enter the cortex in *Satb2 cko* brains, and that Satb2 is required for whisker barrel formation and may play a role in proper TCA targeting (Figure 6B).

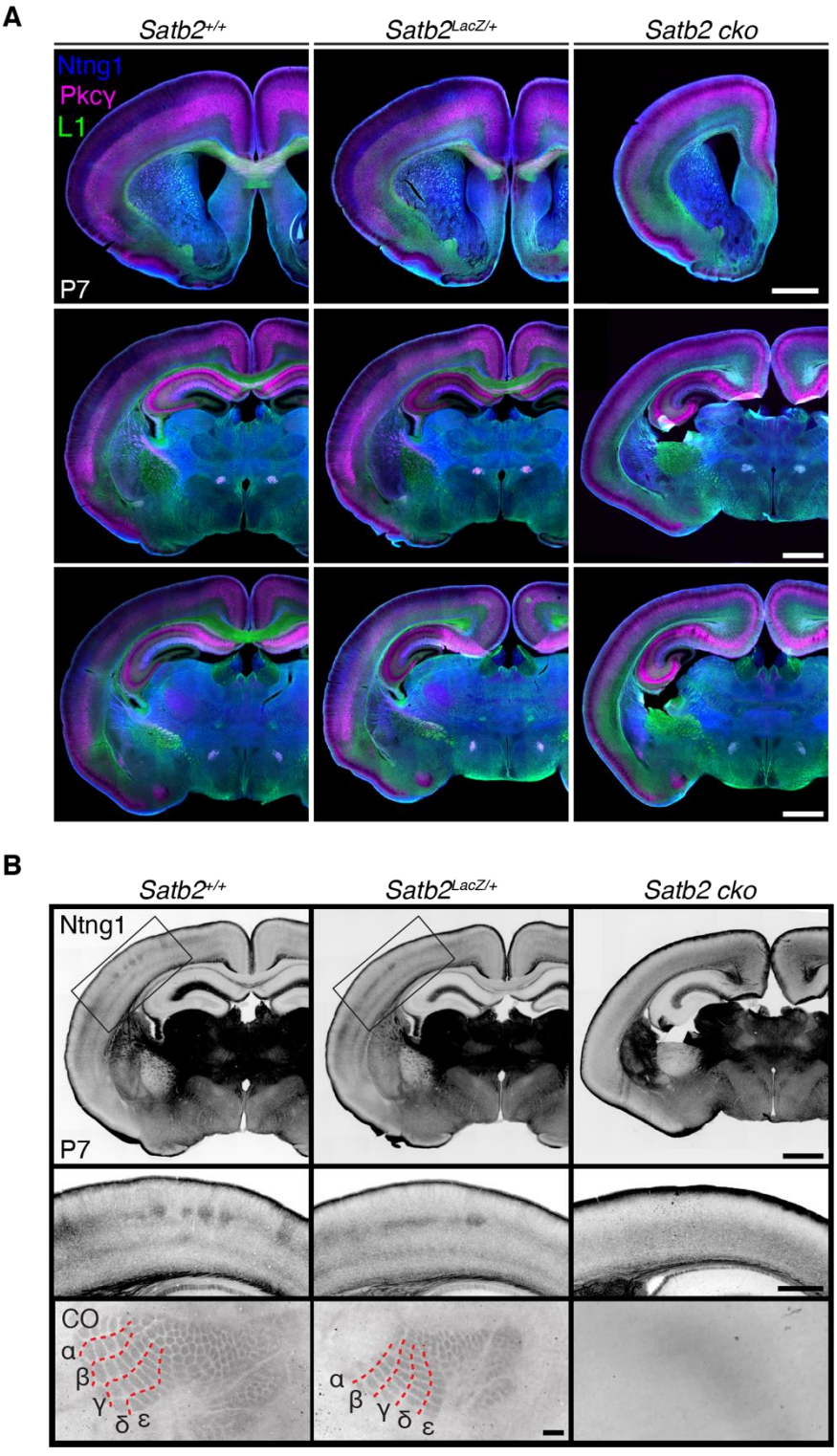
A
Satb2+/+
Satb2LacZ/+
Satb2 cko
Ntng1
Pkcγ
L1
P7
B
Satb2+/+
Satb2LacZ/+
Satb2 cko
Ntng1
P7
CO
α
β
γ
δ
ε

Figure 6: Corpus callosum and thalamocortical projection defects in *Satb2*$^{LacZ/+}$ and *Satb2 cko* cortices

(A) Immunostaining for Ntng1, Pkc γ and L1 in *Satb2*$^{+/+}$, *Satb2*$^{LacZ/+}$, and *Satb2*$^{LacZ/Flox}$; *Emx1*^{Cre} P7 cortices. Scale bars: 1000 µm
(B) Top two rows, Ntng1 staining. High magnification scale bar 1000 µm, low magnification scale bar 500 µm. Bottom row, CO stain on tangential sections at P7. Scale bar 100 µm.

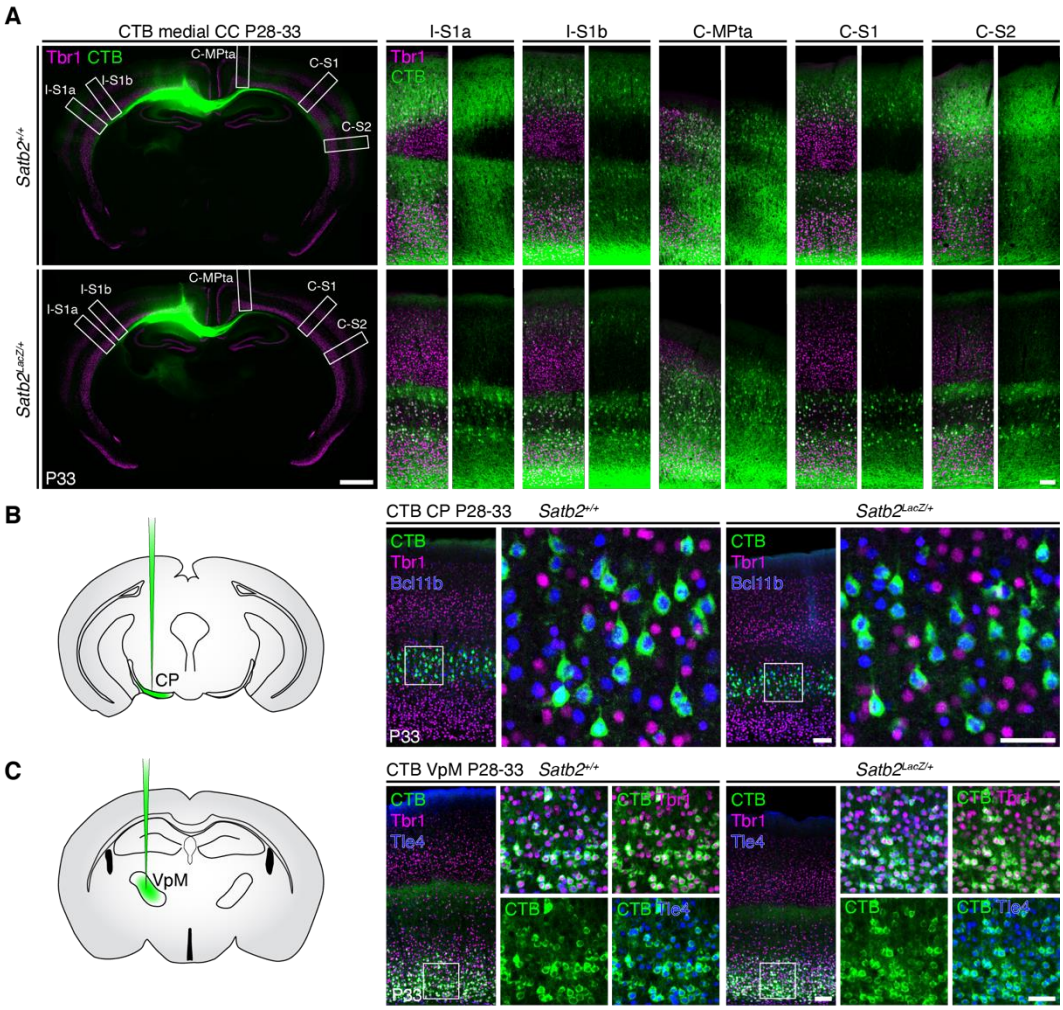

Figure 7: *Satb2*$^{LacZ/+}$ cortices exhibit callosal projection defects and normal subcerebral and corticothalamic axon projections

(A) CtB tracing from the corpus callosum (CC) and staining with Tbr1 to visualize layers. Low magnification scale bar: 1000 µm, high magnification scale bar 100 µm.
(B) Schematic showing injection of CtB into the CP in green. Brains were stained for Tbr1 and Bcl11b. Images taken of S1 regions in *Satb2*$^{+/+}$ and *Satb2*$^{LacZ/+}$ brains. Low magnification scale bar: 100 µm, high magnification scale bar 50 µm
(C) Schematic showing injection of CtB into the VpM. Brains were stained for Tbr1 and Tle4. Images taken of S1 regions in *Satb2*$^{+/+}$ and *Satb2*$^{LacZ/+}$ brains. Low magnification scale bar: 100 µm, high magnification scale bar 50 µm

CUT&RUN analysis reveals Satb2 targets

To identify targets of Satb2, we performed Cleavage Under Targets & Release Using Nuclease (CUT&RUN) (Skene and Henikoff, 2017) experiments using P0 wild-type cortices and antibodies for Satb2 and histone marks associated with active (H3K27Ac And H3K4Me3), and repressive (H3K27Me3) chromatin states (Bannister and Kouzarides, 2011). After mapping sequencing reads to the genome, binding peaks were called using SEACR (Meers et al., 2019) and we identified 8878 Satb2 binding peaks at both promoters (defined as less than 2kb upstream from the transcription start site, TSS), and potential enhancer regions (Figure 8A and 8C). Satb2 binding peaks were enriched with all three histone marks analyzed, indicating that Satb2 interacts with active and repressive chromatin states.

Motif analysis revealed that Satb2 bound promoters are enriched in motifs for transcription activators, including Nfy, Sp2/5/1, and Klf1/5/14/3. Potential enhancer regions are enriched for binding motifs for CTCF and transcription factors (TF) including Neurog2, Neurod1, and Lhx2 (Figure 8A and Figure 8C). The enrichment of motifs for these TFs at Satb2-bound enhancers highlights its role in the development and differentiation of cortical projection neurons.

We identified 5589 Satb2 target genes after associating the Satb2 binding peaks to genes using ChIPseeker (Yu et al., 2015). We combined this information with bulk RNA-seq of P0 *Satb2*$^{LacZ/LacZ}$ cortices (McKenna et al., 2015), and found 360 genes directly repressed and 628 genes directly activated by Satb2. Gene ontology analysis revealed that Satb2 activates genes coding for proteins involved in chromatin remodeling, transcription, and various neurodevelopmental processes, while the Satb2 represses genes encoding proteins related to glial cell development, myelination, and various other biological processes and functions unrelated to cortical development.

Satb2 specifies cell fate, in part, by regulating the expression of post-mitotic transcription factors that are essential for generating various projection neuron subtypes (Alcamo et al., 2008; Britanova et al., 2008b; McKenna et al., 2015). Indeed, we identified

numerous direct Satb2 targets included genes encoding cell fate and layer-specific transcription factors. Layer 5b specific genes that are directly repressed are *Bcl11b*, *Ldb2*, *Grm5*, *Sema5a*, and *Camd1* (Figure 8D). On the other hand, layer-specific genes that are directly activated include deep layer genes *Fezf2, Sox5, Tbr1, Tle4, Wnt7b,* and upper-layer genes *Cux1, Mdga1, Zbtb20,* and *Lhx2* (Figure 8D). These findings highlight the role of Satb2-mediated gene activation and repression for regulating the expression of layer-specific genes and genes involved in a multitude of developmental processes.

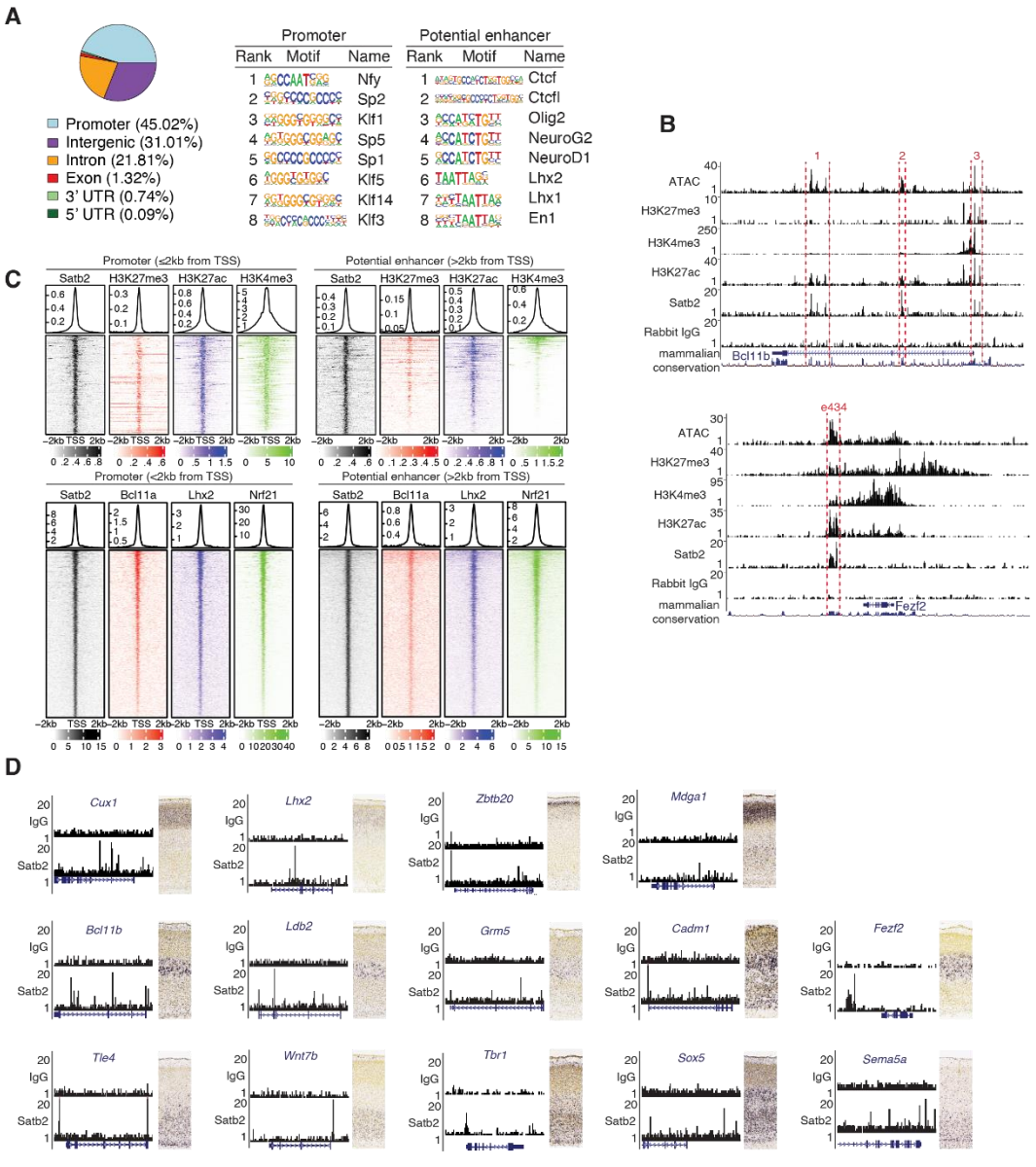
A
Promoter (45.02%)
Intergenic (31.01%)
Intron (21.81%)
Exon (1.32%)
3' UTR (0.74%)
5' UTR (0.09%)
Promoter
Rank Motif Name
1 Nfy
2 Sp2
3 Klf1
4 Sp5
5 Sp1
6 Klf5
7 Klf14
8 Klf3
Potential enhancer
Rank Motif Name
1 Ctcf
2 Ctcfl
3 Olig2
4 NeuroG2
5 NeuroD1
6 Lhx2
7 Lhx1
8 En1
B
ATAC
H3K27me3
H3K4me3
H3K27ac
Satb2
Rabbit IgG
mammalian conservation
Bcl11b
e434
Fezf2
C
Promoter (≤2kb from TSS)
Potential enhancer (>2kb from TSS)
Satb2
H3K27me3
H3K27ac
H3K4me3
Promoter (<2kb from TSS)
Potential enhancer (>2kb from TSS)
Bcl11a
Lhx2
Nrf21
D
Cux1
Lhx2
Zbtb20
Mdga1
Bcl11b
Ldb2
Grm5
Cadm1
Fezf2
Tle4
Wnt7b
Tbr1
Sox5
Sema5a
IgG
Satb2

Figure 8: CUT&RUN reveals Satb2 binding sites

(A) Distribution of Satb2 binding sites and MEME motif analysis. Promoter regions are defined as ≤2kb from transcription start site. Potential enhancer regions are defined as >2kb from transcription start site.
(B) Example UCSC genome browser snapshots showing ATAC track as well as coverage tracks for H3K27me3, H3K27Ac, H3K4me3, Satb2, and Rabbit IgG. Satb2 binding sites are between red dashed lines.
(C) Satb2 binding sites are enriched for histone marks H3K27me3, H3K27Ac, and H3K4me3, and transcription factors Bcl11a, Lhx2, Nr2f1. Explain the scales?
(D) Example UCSC genome browser tracks showing IgG and Satb2 coverage tracks for layer-specific genes. P4 Allen brain atlas in-situ hybridization images are shown to the right of each genome browser graphic. Satb2 activates *Cux1, Mdga1, Zbtb20, Lhx2, Fezf2, Sox5, Tbr1, Tle4,* and *Wnt7b.* Satb2 represses *Bcl11b, Ldb2, Grm5, Sema5a,* and *Camd1*.

Misregulated gene expression due to *Satb2* haploinsufficiency at P28

To understand the impact of *Satb2* haploinsufficiency on gene expression in the cortex, we performed single nuclei RNA sequencing (snRNA-seq) on dissected S1 regions from P28 *Satb2*$^{+/+}$ and *Satb2*$^{LacZ/+}$ cortices. After filtering for quality control, 7865 *Satb2*$^{+/+}$ and 8389 *Satb2*$^{LacZ/+}$ cells were kept for analysis. We co-clustered the *Satb2*$^{+/+}$ and *Satb2*$^{LacZ/+}$ cells (Figure 9A) and performed differential expression analysis to assess the gene expression changes due to *Satb2* haploinsufficiency.

Clusters expressing *Satb2* included L2/3 IT, L6 CT, L6 IT, L4 IT, L4/5 IT, and L5 IT (clusters 0, 1, 2, 5, 7, and 11, respectively). Differential expression analysis within clusters between *Satb2*$^{+/+}$ and *Satb2*$^{LacZ/+}$ cells revealed that the *Satb2* expressing clusters exhibited many significant differentially expressed genes (DEGs, >150). Clusters corresponding to projection neuron subtypes that did not express *Satb2* included, L5NP, L5 PT, and L6b subplate cells (clusters 18, 13, and 20, respectively) had relatively few significant DEGs (<10). Additionally, non-neuronal subtypes such as endothelial cells (cluster 21) exhibited few if any significant DEGs (Figure 9B). This analysis revealed that *Satb2* haploinsufficiency leads to widespread gene misregulation in *Satb2* expressing cell types.

Among the top misregulated genes in *Satb2* expressing cells, were those related to axon guidance, cell adhesion, and ion channels. For example, the following genes were misregulated in two or more *Satb2* expressing clusters and based on CUT&RUN analysis were identified as direct binding targets of Satb2: axon guidance genes *Epha3, Epha7, Gap43, Ppfia2, Slit2, Unc5c*, cell adhesion related genes *Alcam, Cdh10, Cntn3, Cntnap2, Ctnna3, Dock4, Lrfn5, Lsamp, Nectin3, Pcdh9, Sgcz,* and ion channel genes *Cacna1a, Cacna2dl, Kcnd3, Kcnh7, Kcnip3, Kcnip4, Kctd16*. This reveals the critical role of Satb2 in directly regulating genes essential for proper neuronal maturation and function.

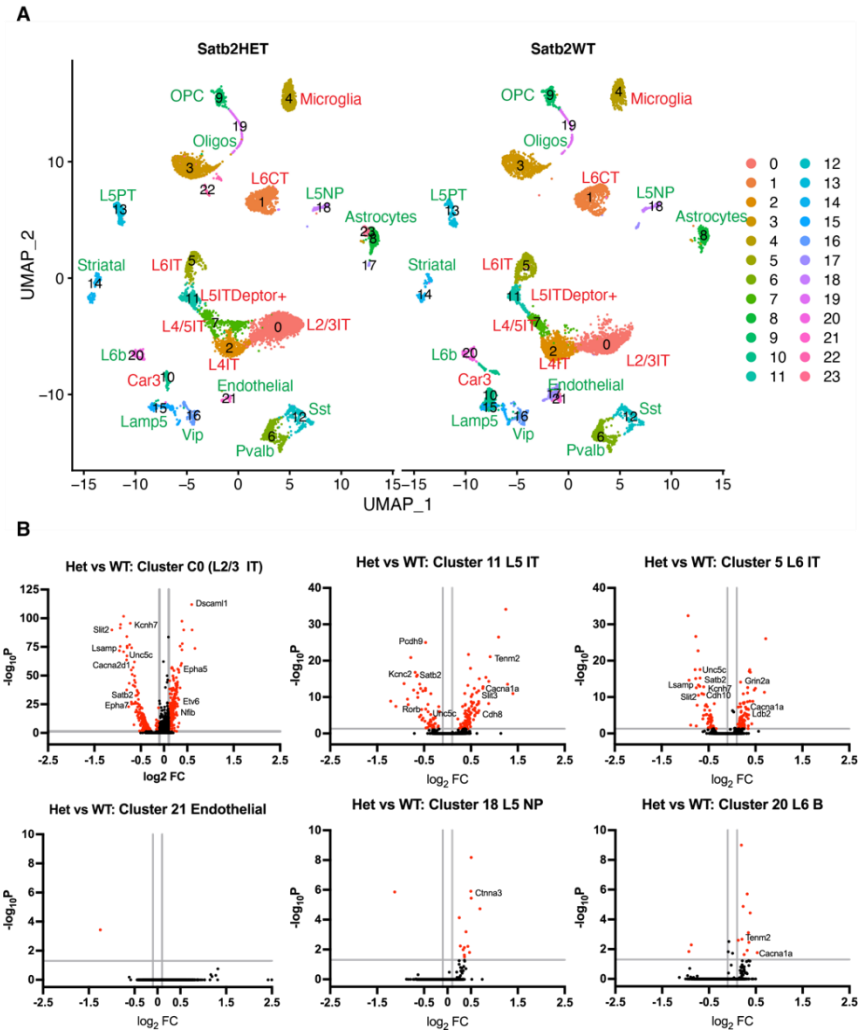

Figure 9: snRNA-seq with S1 P28 tissue reveals widespread misregulated gene expression in *Satb2*$^{LacZ/+}$ cortex

(A) UMAP generated from snRNA-seq from dissected S1 regions in P28 *Satb2*$^{+/+}$ and *Satb2*$^{LacZ/+}$ mice enabled identification of different projection neuron subtypes. Clusters labeled in green showed little to no gene expression changes between *Satb2*$^{+/+}$ and *Satb2*$^{LacZ/+}$ cell types while cells in red exhibited large gene expression changes.
(B) Plots of -$\log_{10}$(p-adjusted value) vs $\log_2$(fold change). Clusters 0, 11, and 6 are Satb2 expressing clusters exhibiting many significant DEGs while clusters 21, 18, and 20 do not express Satb2 and exhibited few significant DEGs. Verticle lines represent $\log_2$(fold change) of ± 0.1 and horizontal lines represent -$\log_{10}$(p-adjusted value = 0.05)

Satb2 haploinsufficiency results in altered electrophysiology of layer 5 neurons and local circuit defects

We performed whole-cell patch-clamp recordings on layer 5 neurons to investigate the impact of *Satb2* haploinsufficiency on the functional development of layer 5 neurons in S1 at P28 (FigureA-10D). We found that *Satb2*$^{LacZ/+}$ neurons exhibited increased rheobase current, wider action potential (AP) half width, and decreased AP firing in response to depolarizing current steps compared to control neurons (Figure 10A and 10C). There was no change in AP threshold or membrane resistance (Figure 10A and 10B). Our recording showed significantly decreased amplitude and frequency of mEPSCs for these neurons (Figure 10D). These data indicate that the S1 L5 projection neurons in *Satb2*$^{LacZ/+}$ mice are intrinsically less excitable.

To determine the impact of *Satb2* haploinsufficiency on local cortical circuitry at P28, we applied laser scanning photostimulation (LSPS), which allows for high throughput functional readout of local circuit connectivity with cellular resolution, and glutamate uncaging to map circuit connectivity (Figure 10F and 10E) (Dantzker and Callaway, 2000; Qiu et al., 2011; Shepherd, 2005; Suter, 2010). We found that S1BF regions of *Satb2*$^{LacZ/+}$ brain slices exhibited disrupted topology of intracortical excitatory connectivity; inputs from layer 4 are reduced while inputs from layer 2/3 are increased, and inhibitory inputs are unchanged (Figure 10F). These data indicate that *Satb2* haploinsufficiency leads to disrupted local excitatory circuit function in S1, potentially due to mis regulated ion channel genes.

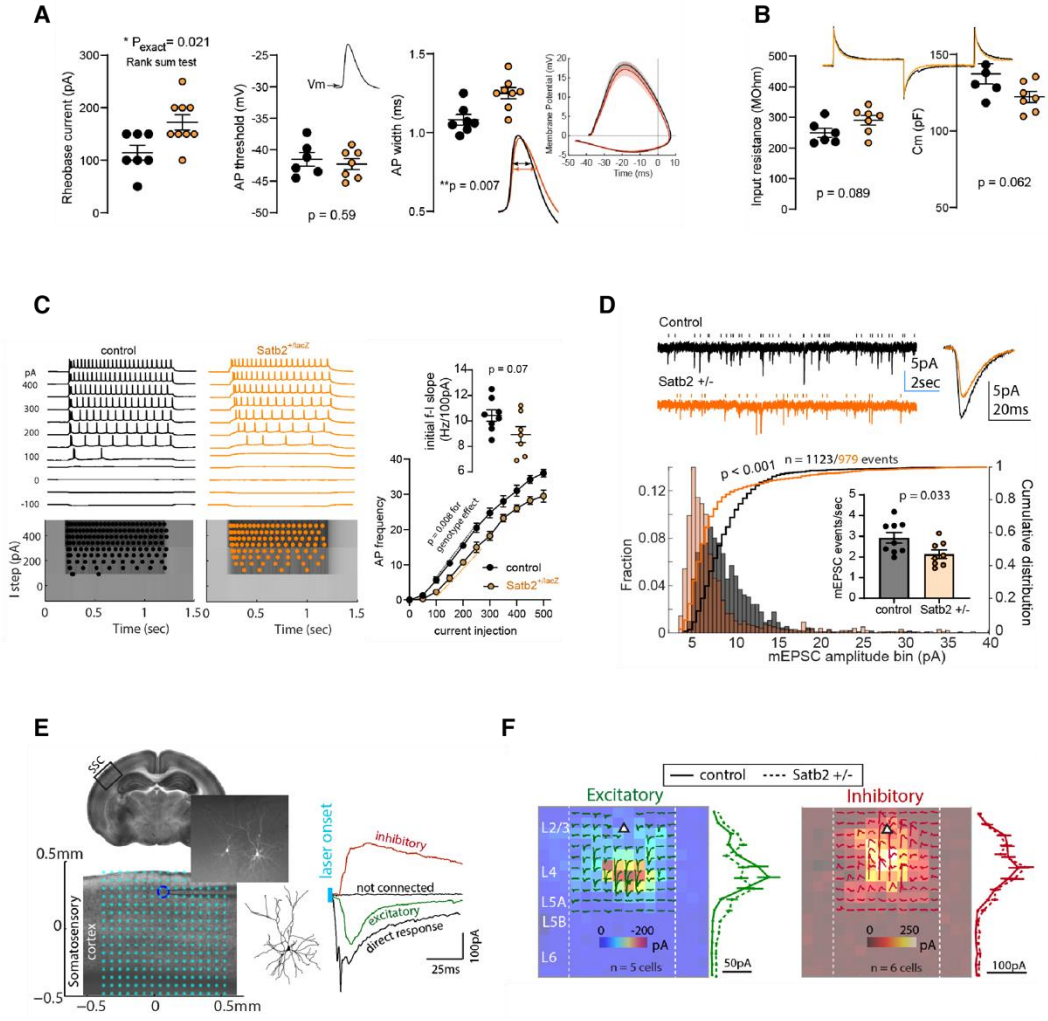
A
* P exact = 0.021
Rank sum test
Rheobase current (pA)
AP threshold (mV)
Vm
p = 0.59
AP width (ms)
**p = 0.007
Membrane Potential (mV)
Time (ms)
B
Input resistance (MOhm)
p = 0.089
Cm (pF)
p = 0.062
C
control
Satb2+/lacZ
I step (pA)
Time (sec)
initial f-I slope (Hz/100pA)
p = 0.07
p = 0.008 for genotype effect
AP frequency
control
Satb2+/lacZ
current injection
D
Control
Satb2 +/-
5pA
2sec
5pA
20ms
p < 0.001
n = 1123/979 events
Fraction
Cumulative distribution
mEPSC amplitude bin (pA)
mEPSC events/sec
p = 0.033
control
Satb2 +/-
E
SSC
0.5mm
0
−0.5
Somatosensory cortex
laser onset
inhibitory
not connected
excitatory
direct response
100pA
25ms
F
control
Satb2 +/-
Excitatory
Inhibitory
L2/3
L4
L5A
L5B
L6
0
-200
pA
n = 5 cells
50pA
0
250
pA
n = 6 cells
100pA

Figure 10: Altered physiology and local circuit connectivity in *Satb2*$^{LacZ/+}$ brain slices

(A) Increased Rheobase current indicating significantly higher current is needed to elicit *Satb2*$^{LacZ/+}$ layer 5 axon potential. No change in action potential threshold. Increased AP width and altered waveforms.
(B) Input resistance and membrane capacitance not significantly changed.
(C) Sample responses of membrane voltages to increasing depolarizing current injections in Satb2+/+ and Satb2LacZ/+ neurons. AP density plots are presented below. Satb2LacZ/+ neurons show significantly lower AP firing in response to current injection indicating reduced excitability.
(D) Sample mEPSC responses from control and Satb2LacZ/+ neurons. Vertical ticks indicate detected mEPSCs. Below is the amplitude distribution and cumulative distribution of mEPSCs. Satb2 LacZ/+ neurons exhibit smaller mEPSC amplitude and reduced frequency.
(E) Illustration of recording L2/3 pyramidal neuron location, and LSPS mapping glutamate uncaging locations. Representative L2/3 neuron morphology shown. Graph showing laser onset and different responses based on uncaging locations.
(F) Pooled responses of EPSC/IPSC maps. Averaged responses from 5-6 neurons. Average synaptic responses (mean ± SD) binned by laminar location to the right of the color maps showing different distribution patterns for excitatory maps but not inhibitory. (n = 4 *Satb2*$^{+/+}$, n = 3 *Satb2*$^{LacZ/+}$ mice)

Satb2 regulates gene expression in part by recruiting the BAF complex

Although the mechanism of Satb2 mediated gene repression is known (Britanova et al., 2008a), it is unclear how Satb2 activates gene expression. We performed protein co-immunoprecipitation (co-IP) using a Satb2 antibody and protein extracts from P0 *Satb2*$^{+/+}$ cortices and confirmed that Satb2 interacts with NuRD components HDAC1 and MTA1/2 (data not shown). We investigated the possibility that Satb2 interacts with the BAF complex, an ATP-dependent chromatin remodeling complex generally associated with gene activation. We found Brg1, the core ATPase in the BAF complex, was co-IPed with a Satb2 antibody from *Satb2*$^{+/+}$, but not *Satb2*$^{LacZ/LacZ}$ cortices (Figure 11A). We also performed the reverse co-IPs, and found a Brg1 antibody, but not a control IgG, was able to co-IP Satb2 from control cortices. Supporting this finding, a co-IP experiment followed by mass spectrometry using a Brg1 antibody with extracts from a primary cortical neuron culture, identified Satb2 as one of the top enriched proteins (data not shown). Immunostaining confirmed their co-expression in the cortical plate (Figure 11B). This interaction highlights the dynamic mechanisms by which Satb2 mediates gene regulation.

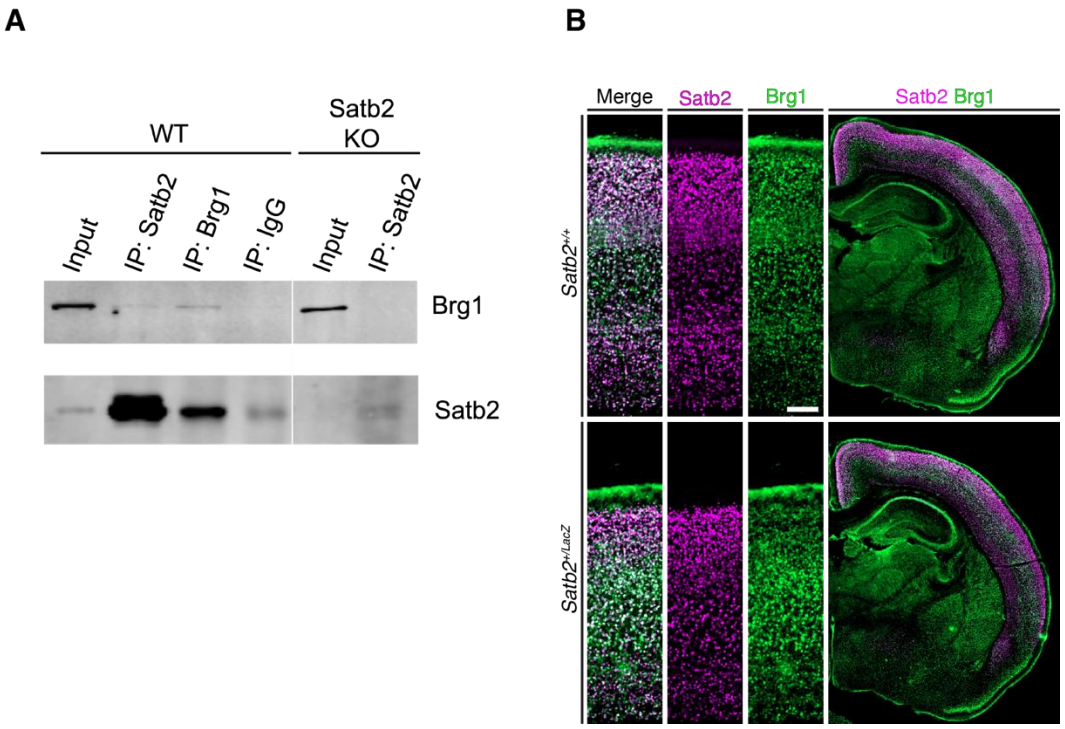

Figure 11: Satb2 and Brg1 can bind to each other and are co-expressed in the cortical plate

(A) Co-immunoprecipitation experiment showed that Satb2 and Brg1 can bind to each other. Satb2 and Brg1 are co-IPed from P0 *Satb2*$^{+/+}$ cortices using either a Brg1 or Satb2 antibody, but not from *Satb2*$^{LacZ/LacZ}$ cortices. Note that there was a non-specific band that co-IPed with control IgG that ran the size of Satb2, and the non-specific band was also co-IPed in *Satb2*$^{LacZ/LacZ}$ cortices.
(B) Satb2 and Brg1 staining revealed that they are co-expressed in cortical neurons in the cortical plate at P7.

Discussion

Understanding the genetic and molecular origin of neurodevelopmental disorders entails deciphering the detailed molecular mechanisms underlying brain development. The molecular and genetic interplay underpinning the generation of cortical projection neurons is beginning to be unraveled, but a comprehensive understanding of these processes is needed. These data shed light on the necessity of proper Satb2 expression for the generation and development of cortical projection neurons. We show that in the *Satb2*$^{LacZ/+}$ animals, there is a 50% reduction of Satb2 protein which leads to widespread gene misregulation, particularly of cell adhesion, axon guidance, and ion channel genes, providing potential a mechanism underlying the axon projection and electrophysiology defects observed. The reduction of Satb2 still permitted the specification of cortical projection neuron classes, yet the insufficient protein levels resulted in severe callosal projection neuron defects. This finding is analogous to the corpus callosum agenesis seen in human SAS patients and provides a molecular mechanism for this pathology.

Previous studies using complete or conditional *Satb2* knockouts, precluded the ability to examine the role of Satb2 in neuronal subtypes that are completely missing in these models. The *Satb2*^{LacZ} allele allowed us to study the role of Satb2 in neuronal maturation, a process distinct from the initial cell fate specification. We confirmed that Satb2 is expressed in CT neurons (McKenna et al., 2015) and found that there are no apparent CT targeting defects in the *Satb2*$^{LacZ/+}$ cortices. However, the layer 6 CT neurons exhibited significant gene expression changes by P28 indicating defective development of these cell types. Interestingly the layer 5 pyramidal tract (PT) neurons showed no apparent gene expression or projection defects in the *Satb2*$^{LacZ/+}$ brain, despite Satb2 being necessary for their birth and specification (Leone et al., 2015b; McKenna et al., 2015). Satb2 expression in the layer 5 PT neurons is transient, and high levels of Fezf2 extinguish Satb2 expression in this neuronal subtype (Chen et al., 2008b; McKenna et al., 2015). Therefore, reduced Satb2 is sufficient to specify the proper number of these neurons which were ultimately unaffected by *Satb2* haploinsufficiency. Satb2 is also

required for the specification of callosal neurons, and its expression is maintained in this cell population after the neurons are born. Although markers of upper-layer projection neurons appeared mostly normal in our immunohistochemistry analysis, gene expression defects were prevalent in our snRNA-seq experiment and callosal projection defects were severe. These findings implicate that Satb2 dosage to be a critical factor in facilitating neuronal maturation. The subtypes of neurons most affected by *Satb2* haploinsufficiency are those that express Satb2 long term, suggesting that IT and CT neuronal subtypes are particularly vulnerable to deficient levels of Satb2. This highlights the vulnerable cell types in SAS.

Satb2 regulates the generation of multiple neuronal subtypes. The question then arises of how Satb2 functions in distinct but essential ways in different projection neuron subtypes. Our findings suggest that the combinatorial action of Satb2 with ATP-dependent chromatin remodeling complexes is one mechanism by which Satb2 regulates gene expression in a cell-context dependent manner. We confirmed previous findings that Satb2 interacts with the NuRD nucleosome remodeling complex which inhibits gene expression through its deacetylase activity (Hoffmann and Spengler, 2019). We found that Satb2 also interacts with the BAF complex which utilizes ATP to mobilize nucleosomes resulting in increased chromatin accessibility (Sokpor et al., 2017), providing a mechanism by which Satb2 activates gene expression. Our CUT&RUN analysis revealed that Satb2 binding sites are enriched for transcription factor binding sites including Bcl11a, Lhx2, and Nr2f1. These findings suggest that the combinatorial action of Satb2 with other chromatin remodeling complexes and transcription factors facilitates its cell-context dependent functions.

Mutations in a single copy of *SATB2* resulting in a nonfunctional SATB2 protein cause Satb2-Associated Syndrome (Zarate and Fish, 2017). SATB2 function is also implicated in autism, schizophrenia, and intellectual deficiency (Blumenthal et al., 2014; Ripke et al., 2014; Whitton et al., 2018). Our findings highlight how projection neuron development is sensitive to Satb2 dosage, particularly in neurons that express Satb2 after their birth and specification. In the *Satb2*$^{LacZ/+}$ brain it appears that the major detrimental effects are due to improper

maturation. This opens the possibility for therapies aimed at SAS that do not have to be implemented during early neonatal development. Finally, this work illuminates the function of Satb2 in heathy brains and sheds light on the etiology of SAS in particular cell types.

Mice used in this study

Experiments were performed according to protocols approved by the Institutional Animal Care and Use Committee at University of California at Santa Cruz and at University of Arizona College of Medicine Phoenix, and were performed in accordance with institutional and federal guidelines.

The *Satb2*$^{LacZ/+}$, and *Emx1*^{Cre}, reporter mice were described previously (Dobreva et al., 2003; Gorski et al., 2002). The *Satb2*$^{tm1a(KOMP)Wtsi/+}$ mice were obtained from the Knockout Mouse Project (KOMP) repository and bred with *Rosa26Sortm2(FLP*)Sor* mice from the Jackson Laboratory (JAX number 007844) to generate the *Satb2*$^{flox(KOMP)/+}$ mice (referred as *Satb2*^{flox} mice in this study).

The day of the vaginal plug detection was designated as E0.5. The day of birth was designated as P0. The genders of the embryonic and early postnatal mice were not determined. The following mice were used in this study:

Satb2$^{+/+}$, *Satb2*$^{LacZ/+}$ and *Satb2*$^{LacZ/LacZ}$ mice: E13.5, E15.5, E17.5, P0, P1, P4, P7, P28, and adult, both male and female mice were used.

Satb2$^{flox/LacZ}$;*Emx1*$^{cre/+}$ mice: P7 and adult, both male and female mice were used.

Method Details

Immunohistochemistry

To prepare tissue for staining, mice were first anesthetized and prepared for trans-cardiac perfusion. 1XPBS was delivered to the body into the left ventricle. When the fluid exiting the right atrium ran clear, 4% paraformaldehyde was pumped until the body stiffened. Brains

were then dissected and post-fixed in 4% paraformaldehyde, 0.1% saponin, 1XPBS for 24 hours at 4°C and then cryoprotected by submerging in 30% sucrose 1XPBS for 24 hours. The brains were sectioned using a sliding microtome into 50µm sections. Sections were permeabilized with 0.06% Triton X-100 in PBS for 30 minutes before incubated in blocking buffer (5% horse serum, 0.03% Triton X-100, 1XPBS) for 1 hour. Blocking buffer was removed, and the sections were incubated with primary antibodies diluted in blocking buffer for 24 hours at 4°C. The following antibodies were used for immunohistochemistry in this study: Bcl11b, 1:1000 (rat, Abcam, ab18465) Brg1, 1:500 (mouse, Santa Cruz Biotechnology, sc-17796), Cux1, 1:500 (rabbit, Santa Cruz Biotechnology, sc-6327), Lhx2, 1:500 (goat, Santa Cruz Biotechnology, sc-19344), L1, 1:500 (rat, MilliporeSigma, MAB5272), Ntng1 1:100 (goat, R&D Systems, AF1166), Pkcg, 1:500 (rabbit, Santa Cruz Biotechnology, sc-211), Rorb (rabbit, Proteintech 17635-1-AP), Satb2, 1:1000 (rabbit, Abcam, ab34735), Tbr1 (rabbit, Abcam, ab31940), Tbr2, 1:500 (rat, Abcam, ab23345), Tle4, 1:100 (mouse, Santa Cruz Biotechnology, sc-365406). The sections were washed three times with 1XPBS 0.03% triton X-100 for 5 minutes each, and then incubated with secondary antibodies conjugated to Alexa 488, 555, or 647 fluorophores, all diluted in blocking buffer at a ratio of 1:1000. Secondary antibodies were incubated for 2 hours at room temperature. Nuclear staining was performed by incubating with 4',6-Diamidino-2-Phenylindole, Dihydrochloride (DAPI) 1:10,000 (Invitrogen, D1306) in 1XPBS for 10 minutes. Sections were then manually arranged on microscope slides before being mounted in Fluoromount-G. Embryonic tissue was sectioned at 20µm using a Leica Cryostat, and staining was performed as described above but on microscope slides.

Cytochrome oxidase staining

Brains used for cytochrome oxidase staining were dissected from perfused mice as described in the “Immunohistochemistry” methods section. Brains were cut in half along the midline and all subcortical structures were removed with standard dissecting tools to obtain cortices. We then flattened the cortices between two glass slides with a 1mm spacer in-

between and placed in 4%PFA 1XPBS 0.1% saponin at 4°C overnight and then cryoprotected by submerging in 30% sucrose 1XPBS for 24 hours. The flattened cortices were then sectioned on a sliding microtome at 50µm. Sections were washed with 1X PBS and then incubated at 37°C in CO staining buffer containing: 5% sucrose, 0.03% cytochrome C, 0.02% catalase, 0.05% 3,3′-Diaminobenzidine, and 0.1M phosphate buffer for 2-3 hours. Sections were then washed with 1X PBS and mounted in Permount.

EdU labeling

Timed pregnant mice were injected with a single dose of EdU (25mg/kg body weight; Thermo Fisher Scientific, E10187) at E12.5, or E13.5. Brains were collected at P7 as described in "immunohistochemistry." Primary and secondary antibody staining was performed as usual, and at the end of the protocol, sections were immersed in the following solution 1 mL of reaction: 950ul 100mM Tris PH 7.4, 40µL 100 mM $CuSO_4$, 10µL 200 mg/mL sodium ascorbate, and 1µL azide 488 or 555 at room temperature for 30 minutes. Sections were then washed and cover slipped. *Satb2*$^{LacZ/+}$ and littermate *Satb2*$^{+/+}$ control mice were analyzed for each timepoint.

CUT&RUN

P0 brains were quickly dissected and dropped into ice cold 1X PBS with protease inhibitor (Roche 11873580001). Cortices were then dissected under a dissection microscope. The pial surface was carefully removed and the cortices were cut into small pieces. The tissue was then washed with 400µL ice cold Accumax solution (Sigma-Aldrich A7089). Ice cold Accumax was removed and 400µL prewarmed 37°C Accumax was added. The tissue incubated at 37°C for 5 minutes before being manually dissociated with a P1000 pipet tip. Dissociated cells were spun down at 600g for 3 minutes and resuspended in 1mL ice cold wash buffer (20mM HEPES pH 7.5, 150mM NaCl, 0.5mM Spermidine, 1X EDTA-free protease inhibitor). The cells were washed three times. Cells were then quantified and bound to

Concanavalin-A beads (Bangs Laboratories, PB531). All CUT&RUN samples were generated with 500,000 cells. Cells were then bound to beads at a ratio of 500,000 cells per 10µL beads. Cells bound to beads were then placed on a magnetic stand and the wash buffer was removed. Each sample was resuspended in 150µL antibody buffer (wash buffer with 2mM EDTA, 0.03% Digitonin, MilliporeSigma, 300410). All antibodies were used at a dilution of 1:100, except the IgG which was added to a final concentration of 1µg/µL. The following antibodies were used in CUT&RUN experiments: Satb2 (rabbit, Abcam, ab34735), Cux1 (rabbit, Santa Cruz Biotechnology, sc-6327), Lhx2 (goat, Santa Cruz Biotechnology, sc-19344), H3K27me3 (Cell Signaling, 9733S), H3K27Ac (Abcam, Ab4729), H3K4me3 (Cell Signaling, 97515), Rabbit IgG (Invitrogen 02-6102). Samples were incubated at 4°C overnight with shaking a 400rpm at a 30° angle (the tubes were never inverted). The following day, beads were washed twice with 1mL DIG-wash buffer (Wash Buffer with 0.03% Digitonin), and incubated with protein A/G-MNase (EpiCypher, 15-1016), 2.5µL per 50µL DIG-wash buffer per sample, for 1 hour at 4°C shaking. Beads were washed twice with DIG-wash buffer and resuspended in 100µL DIG-wash buffer and Ca^{2+} was added to a final concentration of 1mM and the samples incubated for 1 hour at 0°C in a heat block immersed in an ice water slurry. The reaction was inhibited by adding 100µL 2X STOP buffer (170mM NaCl, 20mM EGTA, 0.05%, 50µg/mL RNAse A, 20µg/mL Glycogen, 250pg *E. coli* Spike-in DNA, EpiCypher 18-1401). Samples were then incubated at 37°C for 30 minutes, and supernatant was transferred to fresh tubes. Phenol chloroform isoamyl alcohol extraction was performed to purify CUT&RUN DNA which was resuspended in 30µL 1mM Tris-HCl pH 8.0, 0.1mM EDTA.

CUT&RUN Library Prep and Sequencing and Analysis

We used the NEBNext Ultra II DNA Library Prep Kit (E7645L) with some modifications to the protocol. For the adapter ligation step, the NEBNext Adaptor for Illumina was diluted 1:50, to 0.3µM. The adaptor ligated DNA was then cleaned up with 2.1X AMPure XP beads

(Beckman A63881) before proceeding. PCR was performed with NEBNext Multiplex Oligos for Illumina (E7600S) with the following thermocycler conditions: Initial denaturation 98°C, 30s, denaturation 98°C, 10s, annealing and extension 65°C, 12s, repeat denaturing and annealing and extension 14 times, final extension 65°C, 5 minutes in a Bio-Rad T100 Thermal Cycler. After amplification, 0.5X AMPure beads were added to the reaction, mixed, incubated for 10 minutes, and samples were placed on a magnet stand. Supernatant was transferred to fresh tubes and then cleaned up with 2X AMPure beads. DNA concentrations were determined using Bioanalyzer High Sensitivity DNA kit (5067-4626). DNA between 146 and 600bp was quantified for the analysis. The primer-dimer peak was removed with Pippin size selection. Samples were pooled such that equimolar amounts of each sample were present in the pool, and sequenced on the NextSeq platform (high output, 75 cycles). The sequencing was demultiplexed, and sequencing reads were mapped to the genome. Binding peaks were called using SEACR, and peaks were assigned to genes using ChIPseeker. MEME motif analysis was used to determine Satb2 binding motifs.

snRNAseq

P28 mice were anesthetized and brains were quickly dissected and placed into ice cold PBS. The brains were then sectioned at 300 µm using a vibratome. S1 regions were then manually excised from the brain sections and flash frozen in liquid nitrogen. Nuclei were then isolated and libraries made using the 10X genomics single cell gene expression workflow. Libraries were sequenced on the NovaSeq platform. Quality control analysis was performed using the Seurat workflow. Harmony (Korsunsky et al., 2019) to co-cluster the datasets and perform differential expression analysis.

CtB labeling

Injections for tracing experiments were performed using Alexa Fluor 555-conjugated cholera toxin subunit-B (CtB) at a concentration of 4 mg/mL in 1XPBS injected through a pulled glass pipet attached to a Picospritzer III (Parker). Stereotaxic surgery was performed on P28 mice by anesthetizing them and placing on a stereotaxic frame (Kopf). The skull was exposed, and coordinates were measured by using the bregma as the zero point. A craniotomy was performed, and the pulled glass pipet with CtB was placed on the brain surface. The needle was then lowered to the desired Z position, and 0.25µL was injected. After 5 minutes, the needle was retracted, and the skin was glued back together. Brains were analyzed 5-days later. Injections were performed using the following coordinates: VpM injection, AP -1 mm, ML 2.85 mm, Z -3.35 mm, CP injection AP -3.28 mm, ML 1.3 mm, Z -4.8 mm, CC injection AP -1.7 mm, ML 0.8 mm, Z -1.3 mm.

Image acquisition and analysis

Images for quantitative analysis were acquired with a Zeiss 880 confocal microscope. Laser power and gain were adjusted until < 1% of pixels were saturated. Cell counting was performed on single z-slices. Images were divided into 500 µm wide regions and split into equally sized bins or cortical layers. A gaussian blur was applied to the image with a rolling ball radius of 1µm and then an appropriate threshold was set for each channel. Particles were analyzed with a circularity of 0.3-1.0 and size exclusion of > 1µm. The same threshold was used across all images between genotypes. Brightfield images were acquired with a Zeiss AxioImager Z2 widefield microscope with a Zeiss AxioCam 506 (color) camera.

Statistical analysis was performed using GraphPad Prism 9.0. For each brain, the number of marker+ cells in the cortex were quantified in a 500 µm wide region from at least 3-4 matching sections. Care was taken to match the anterior-posterior, medial-lateral positions for the chosen areas between the mutant and control genotypes. For each genotype and each age, at least 3 different brains were analyzed. Data are shown as mean ± SEM. Statistical

significance for single comparisons was determined using a nested t-test. Significance was set as $*$ for $p < 0.05$, $**$ for $p < 0.01$, and $***$ $p < 0.001$ for all significance tests.

Western blot analysis

P0 cortices were dissected in ice cold 1X PBS with protease inhibitor. The tissue was homogenized in RIPA buffer by manually triturating with a P1000 pipet tip before incubating on ice for 20 minutes. The cell homogenate was centrifuged at 14,000 g for 10 minutes at 4°C. The supernatant was removed, and proteins were denatured at 100°C for 5 minutes in laemmli buffer. The sample was then run on an 8% SDS-PAGE at 70V for 2 hours, transferred to a PVDF membrane (Sigma, IPVH85R) at 150 mA for 90 minutes. The PVDF was blocked for one hour in 1% non-fat milk in 1X Tris-Buffered Saline, 0.1% Tween 20 (TBST). After blocking in 10mL solution, 2µg Satb2 antibody (rabbit, Abcam, ab34735) was added and incubated at 4°C overnight. The blot was then washed with TBST and incubated in Li-Cor Donkey anti Rabbit secondary antibody (#926-68073) at a 1:17,000 dilution for one hour and images were processed using ImageStudioLite.

References:

Alcamo, E.A., Chirivella, L., Dautzenberg, M., Dobreva, G., Fariñas, I., Grosschedl, R., McConnell, S.K., 2008. Satb2 regulates callosal projection neuron identity in the developing cerebral cortex. Neuron 57, 364–377. https://doi.org/10.1016/j.neuron.2007.12.012

Allen, N.J., Lyons, D.A., 2018. Glia as architects of central nervous system formation and function. Science 362, 181–185. https://doi.org/10.1126/science.aat0473

Azevedo, F.A.C., Carvalho, L.R.B., Grinberg, L.T., Farfel, J.M., Ferretti, R.E.L., Leite, R.E.P., Filho, W.J., Lent, R., Herculano-Houzel, S., 2009. Equal numbers of neuronal and nonneuronal cells make the human brain an isometrically scaled-up primate brain. J. Comp. Neurol. 513, 532–541. https://doi.org/10.1002/cne.21974

Bannister, A.J., Kouzarides, T., 2011. Regulation of chromatin by histone modifications. Cell Res. 21, 381–395. https://doi.org/10.1038/cr.2011.22

Baranek, C., Dittrich, M., Parthasarathy, S., Bonnon, C.G., Britanova, O., Lanshakov, D., Boukhtouche, F., Sommer, J.E., Colmenares, C., Tarabykin, V., Atanasoski, S., 2012. Protooncogene Ski cooperates with the chromatin-remodeling factor Satb2 in specifying callosal neurons. Proc. Natl. Acad. Sci. 109, 3546–3551. https://doi.org/10.1073/pnas.1108718109

Bengani, H., Handley, M., Alvi, M., Ibitoye, R., Lees, M., Lynch, S.A., Lam, W., Fannemel, M., Nordgren, A., Malmgren, H., Kvarnung, M., Mehta, S., McKee, S., Whiteford, M., Stewart, F., Connell, F., Clayton-Smith, J., Mansour, S., Mohammed, S., Fryer, A., Morton, J., Grozeva, D., Asam, T., Moore, D., Sifrim, A., McRae, J., Hurles, M.E., Firth, H.V., Raymond, F.L., Kini, U., Nellåker, C., FitzPatrick, D.R., 2017. Clinical and molecular consequences of disease-associated de novo mutations in SATB2. Genet. Med. 19, 900–908. https://doi.org/10.1038/gim.2016.211

Bissell, S., Oliver, C., Moss, J., Heald, M., Waite, J., Crawford, H., Kothari, V., Rumbellow, L., Walters, G., Richards, C., 2022. The behavioural phenotype of SATB2-associated syndrome: a within-group and cross-syndrome analysis. J. Neurodev. Disord. 14, 25. https://doi.org/10.1186/s11689-022-09426-0

Blumenthal, I., Ragavendran, A., Erdin, S., Klei, L., Sugathan, A., Guide, J.R., Manavalan, P., Zhou, J.Q., Wheeler, V.C., Levin, J.Z., Ernst, C., Roeder, K., Devlin, B., Gusella, J.F., Talkowski, M.E., 2014. Transcriptional consequences of 16p11.2 deletion and duplication in mouse cortex and multiplex autism families. Am. J. Hum. Genet. 94, 870–883. https://doi.org/10.1016/j.ajhg.2014.05.004

Bonilla-Claudio, M., Wang, J., Bai, Y., Klysik, E., Selever, J., Martin, J.F., 2012. Bmp signaling regulates a dose-dependent transcriptional program to control facial skeletal development. Development 139, 709–719. https://doi.org/10.1242/dev.073197

Britanova, O., Akopov, S., Lukyanov, S., Gruss, P., Tarabykin, V., 2005. Novel transcription factor Satb2 interacts with matrix attachment region DNA elements in a tissue-specific manner and demonstrates cell-type-dependent expression in the developing mouse CNS: A novel transcription factor interacting with MARs. Eur. J. Neurosci. 21, 658–668. https://doi.org/10.1111/j.1460-9568.2005.03897.x

Britanova, O., de Juan Romero, C., Cheung, A., Kwan, K.Y., Schwark, M., Gyorgy, A., Vogel, T., Akopov, S., Mitkovski, M., Agoston, D., Sestan, N., Molnár, Z., Tarabykin, V., 2008a. Satb2 is a postmitotic determinant for upper-layer neuron specification in the neocortex. Neuron 57, 378–392. https://doi.org/10.1016/j.neuron.2007.12.028

Britanova, O., De Juan Romero, C., Cheung, A., Kwan, K.Y., Schwark, M., Gyorgy, A., Vogel, T., Akopov, S., Mitkovski, M., Agoston, D., Šestan, N., Molnár, Z., Tarabykin, V., 2008b. Satb2 Is a Postmitotic Determinant for Upper-Layer Neuron Specification in the Neocortex. Neuron 57, 378–392. https://doi.org/10.1016/j.neuron.2007.12.028

Britanova, O., Depew, M.J., Schwark, M., Thomas, B.L., Miletich, I., Sharpe, P., Tarabykin, V., 2006. Satb2 Haploinsufficiency Phenocopies 2q32-q33 Deletions, whereas Loss Suggests a Fundamental Role in the Coordination of Jaw Development. Am. J. Hum. Genet. 79, 668–678. https://doi.org/10.1086/508214

Burns, K.A., Murphy, B., Danzer, S.C., Kuan, C.-Y., 2009. Developmental and post-injury cortical gliogenesis: A Genetic fate-mapping study with Nestin-CreER mice. Glia 57, 1115–1129. https://doi.org/10.1002/glia.20835

Cadwell, C.R., Bhaduri, A., Mostajo-Radji, M.A., Keefe, M.G., Nowakowski, T.J., 2019. Development and Arealization of the Cerebral Cortex. Neuron 103, 980–1004. https://doi.org/10.1016/j.neuron.2019.07.009

Chen, B., Schaevitz, L.R., McConnell, S.K., 2005. Fezl regulates the differentiation and axon targeting of layer 5 subcortical projection neurons in cerebral cortex. Proc. Natl. Acad. Sci. 102, 17184–17189. https://doi.org/10.1073/pnas.0508732102

Chen, B., Wang, S.S., Hattox, A.M., Rayburn, H., Nelson, S.B., McConnell, S.K., 2008a. The Fezf2-Ctip2 genetic pathway regulates the fate choice of subcortical projection neurons in the developing cerebral cortex. Proc. Natl. Acad. Sci. U. S. A. 105, 11382–11387. https://doi.org/10.1073/pnas.0804918105

Chen, B., Wang, S.S., Hattox, A.M., Rayburn, H., Nelson, S.B., McConnell, S.K., 2008b. The *Fezf2–Ctip2* genetic pathway regulates the fate choice of subcortical projection neurons in the developing cerebral cortex. Proc. Natl. Acad. Sci. 105, 11382–11387. https://doi.org/10.1073/pnas.0804918105

Chen, J.-G., Rašin, M.-R., Kwan, K.Y., Šestan, N., 2005. Zfp312 is required for subcortical axonal projections and dendritic morphology of deep-layer pyramidal neurons of the cerebral cortex. Proc. Natl. Acad. Sci. 102, 17792–17797. https://doi.org/10.1073/pnas.0509032102

Clark, E.A., Rutlin, M., Capano, L., Aviles, S., Saadon, J.R., Taneja, P., Zhang, Q., Bullis, J.B., Lauer, T., Myers, E., Schulmann, A., Forrest, D., Nelson, S.B., 2020. Cortical RORβ is required for layer 4 transcriptional identity and barrel integrity. eLife 9, e52370. https://doi.org/10.7554/eLife.52370

Dantzker, J.L., Callaway, E.M., 2000. Laminar sources of synaptic input to cortical inhibitory interneurons and pyramidal neurons. Nat. Neurosci. 3, 701–707. https://doi.org/10.1038/76656

Di Bella, D.J., Habibi, E., Stickels, R.R., Scalia, G., Brown, J., Yadollahpour, P., Yang, S.M., Abbate, C., Biancalani, T., Macosko, E.Z., Chen, F., Regev, A., Arlotta, P., 2021.

Molecular logic of cellular diversification in the mouse cerebral cortex. Nature 595, 554–559. https://doi.org/10.1038/s41586-021-03670-5

Dickinson, L., 1992. A tissue-specific MAR/SAR DNA-binding protein with unusual binding site recognition. Cell 70, 631–645. https://doi.org/10.1016/0092-8674(92)90432-C

Dickinson, L.A., Dickinson, C.D., Kohwi-Shigematsu, T., 1997. An Atypical Homeodomain in SATB1 Promotes Specific Recognition of the Key Structural Element in a Matrix Attachment Region. J. Biol. Chem. 272, 11463–11470. https://doi.org/10.1074/jbc.272.17.11463

Dobreva, G., Chahrour, M., Dautzenberg, M., Chirivella, L., Kanzler, B., Fariñas, I., Karsenty, G., Grosschedl, R., 2006a. SATB2 Is a Multifunctional Determinant of Craniofacial Patterning and Osteoblast Differentiation. Cell 125, 971–986. https://doi.org/10.1016/j.cell.2006.05.012

Dobreva, G., Chahrour, M., Dautzenberg, M., Chirivella, L., Kanzler, B., Fariñas, I., Karsenty, G., Grosschedl, R., 2006b. SATB2 is a multifunctional determinant of craniofacial patterning and osteoblast differentiation. Cell 125, 971–986. https://doi.org/10.1016/j.cell.2006.05.012

Dobreva, G., Dambacher, J., Grosschedl, R., 2003. SUMO modification of a novel MAR-binding protein, SATB2, modulates immunoglobulin μ gene expression. Genes Dev. 17, 3048–3061. https://doi.org/10.1101/gad.1153003

Döcker, D., Schubach, M., Menzel, M., Munz, M., Spaich, C., Biskup, S., Bartholdi, D., 2014. Further delineation of the SATB2 phenotype. Eur. J. Hum. Genet. 22, 1034–1039. https://doi.org/10.1038/ejhg.2013.280

Eckler, M.J., Nguyen, T.D., McKenna, W.L., Fastow, B.L., Guo, C., Rubenstein, J.L.R., Chen, B., 2015. Cux2-Positive Radial Glial Cells Generate Diverse Subtypes of Neocortical Projection Neurons and Macroglia. Neuron 86, 1100–1108. https://doi.org/10.1016/j.neuron.2015.04.020

Fish, J.L., Villmoare, B., Köbernick, K., Compagnucci, C., Britanova, O., Tarabykin, V., Depew, M.J., 2011. Satb2, modularity, and the evolvability of the vertebrate jaw: Satb2, modularity, and jaw evolvability. Evol. Dev. 13, 549–564. https://doi.org/10.1111/j.1525-142X.2011.00511.x

FitzPatrick, D.R., 2003. Identification of SATB2 as the cleft palate gene on 2q32-q33. Hum. Mol. Genet. 12, 2491–2501. https://doi.org/10.1093/hmg/ddg248

Galande, S., Dickinson, L.A., Mian, I.S., Sikorska, M., Kohwi-Shigematsu, T., 2001. SATB1 Cleavage by Caspase 6 Disrupts PDZ Domain-Mediated Dimerization, Causing Detachment from Chromatin Early in T-Cell Apoptosis. Mol. Cell. Biol. 21, 5591–5604. https://doi.org/10.1128/MCB.21.16.5591-5604.2001

Galazo, M.J., Sweetser, D., Macklis, J.D., 2022. Tle4 controls both developmental acquisition and postnatal maintenance of corticothalamic projection neuron identity. https://doi.org/10.1101/2022.05.09.491192

Gao, P., Postiglione, M.P., Krieger, T.G., Hernandez, L., Wang, C., Han, Z., Streicher, C., Papusheva, E., Insolera, R., Chugh, K., Kodish, O., Huang, K., Simons, B.D., Luo, L.,

Hippenmeyer, S., Shi, S.-H., 2014. Deterministic Progenitor Behavior and Unitary Production of Neurons in the Neocortex. Cell 159, 775–788. https://doi.org/10.1016/j.cell.2014.10.027

Gorski, J.A., Talley, T., Qiu, M., Puelles, L., Rubenstein, J.L.R., Jones, K.R., 2002. Cortical Excitatory Neurons and Glia, But Not GABAergic Neurons, Are Produced in the Emx1-Expressing Lineage. J. Neurosci. 22, 6309–6314. https://doi.org/10.1523/JNEUROSCI.22-15-06309.2002

Greig, L.C., Woodworth, M.B., Galazo, M.J., Padmanabhan, H., Macklis, J.D., 2013a. Molecular logic of neocortical projection neuron specification, development and diversity. Nat. Rev. Neurosci. 14, 755–769. https://doi.org/10.1038/nrn3586

Greig, L.C., Woodworth, M.B., Galazo, M.J., Padmanabhan, H., Macklis, J.D., 2013b. Molecular logic of neocortical projection neuron specification, development and diversity. Nat. Rev. Neurosci. 14, 755–769. https://doi.org/10.1038/nrn3586

Guo, C., Eckler, M.J., McKenna, W.L., McKinsey, G.L., Rubenstein, J.L.R., Chen, B., 2013. Fezf2 Expression Identifies a Multipotent Progenitor for Neocortical Projection Neurons, Astrocytes, and Oligodendrocytes. Neuron 80, 1167–1174. https://doi.org/10.1016/j.neuron.2013.09.037

Gyorgy, A.B., Szemes, M., De Juan Romero, C., Tarabykin, V., Agoston, D.V., 2008. SATB2 interacts with chromatin-remodeling molecules in differentiating cortical neurons. Eur. J. Neurosci. 27, 865–873. https://doi.org/10.1111/j.1460-9568.2008.06061.x

Hamasaki, T., Leingärtner, A., Ringstedt, T., O'Leary, D.D.M., 2004. EMX2 Regulates Sizes and Positioning of the Primary Sensory and Motor Areas in Neocortex by Direct Specification of Cortical Progenitors. Neuron 43, 359–372. https://doi.org/10.1016/j.neuron.2004.07.016

Han, W., Kwan, K.Y., Shim, S., Lam, M.M.S., Shin, Y., Xu, X., Zhu, Y., Li, M., Sestan, N., 2011. TBR1 directly represses Fezf2 to control the laminar origin and development of the corticospinal tract. Proc. Natl. Acad. Sci. U. S. A. 108, 3041–3046. https://doi.org/10.1073/pnas.1016723108

He, S., Dunn, K.L., Espino, P.S., Drobic, B., Li, L., Yu, J., Sun, J.-M., Chen, H.Y., Pritchard, S., Davie, J.R., 2008. Chromatin organization and nuclear microenvironments in cancer cells. J. Cell. Biochem. 104, 2004–2015. https://doi.org/10.1002/jcb.21485

Hoffmann, A., Spengler, D., 2019. Chromatin Remodeling Complex NuRD in Neurodevelopment and Neurodevelopmental Disorders. Front. Genet. 10.

Huang, Y., Song, N.-N., Lan, W., Hu, L., Su, C.-J., Ding, Y.-Q., Zhang, L., 2013. Expression of Transcription Factor Satb2 in Adult Mouse Brain: Expression of Satb2 in Adult Brain. Anat. Rec. 296, 452–461. https://doi.org/10.1002/ar.22656

Jiang, G., Cui, Y., Yu, X., Wu, Z., Ding, G., Cao, L., 2015. miR-211 suppresses hepatocellular carcinoma by downregulating SATB2. Oncotarget 6, 9457–9466. https://doi.org/10.18632/oncotarget.3265

Keino-Masu, K., Masu, M., Hinck, L., Leonardo, E.D., Chan, S.S.-Y., Culotti, J.G., Tessier-Lavigne, M., 1996. Deleted in Colorectal Cancer (DCC) Encodes a Netrin Receptor. Cell 87, 175–185. https://doi.org/10.1016/S0092-8674(00)81336-7

Kennedy, T.E., Serafini, T., De La Torre, JoséR., Tessier-Lavigne, M., 1994. Netrins are diffusible chemotropic factors for commissural axons in the embryonic spinal cord. Cell 78, 425–435. https://doi.org/10.1016/0092-8674(94)90421-9

Kikuiri, T., Mishima, H., Imura, H., Suzuki, S., Matsuzawa, Y., Nakamura, T., Fukumoto, S., Yoshimura, Y., Watanabe, S., Kinoshita, A., Yamada, T., Shindoh, M., Sugita, Y., Maeda, H., Yawaka, Y., Mikoya, T., Natsume, N., Yoshiura, K., 2018. Patients with SATB2-associated syndrome exhibiting multiple odontomas. Am. J. Med. Genet. A. 176, 2614–2622. https://doi.org/10.1002/ajmg.a.40670

Kikuno, R., 2002. HUGE: a database for human large proteins identified in the Kazusa cDNA sequencing project. Nucleic Acids Res. 30, 166–168. https://doi.org/10.1093/nar/30.1.166

Kim, D., Ackerman, S.L., 2011. The UNC5C Netrin Receptor Regulates Dorsal Guidance of Mouse Hindbrain Axons. J. Neurosci. 31, 2167–2179. https://doi.org/10.1523/JNEUROSCI.5254-10.2011

Korsunsky, I., Millard, N., Fan, J., Slowikowski, K., Zhang, F., Wei, K., Baglaenko, Y., Brenner, M., Loh, P., Raychaudhuri, S., 2019. Fast, sensitive and accurate integration of single-cell data with Harmony. Nat. Methods 16, 1289–1296. https://doi.org/10.1038/s41592-019-0619-0

Kowalczyk, T., Pontious, A., Englund, C., Daza, R.A.M., Bedogni, F., Hodge, R., Attardo, A., Bell, C., Huttner, W.B., Hevner, R.F., 2009. Intermediate Neuronal Progenitors (Basal Progenitors) Produce Pyramidal–Projection Neurons for All Layers of Cerebral Cortex. Cereb. Cortex 19, 2439–2450. https://doi.org/10.1093/cercor/bhn260

Kriegstein, A., Alvarez-Buylla, A., 2009. The Glial Nature of Embryonic and Adult Neural Stem Cells. Annu. Rev. Neurosci. 32, 149–184. https://doi.org/10.1146/annurev.neuro.051508.135600

Kumar, P.P., Purbey, P.K., Ravi, D.S., Mitra, D., Galande, S., 2005. Displacement of SATB1-Bound Histone Deacetylase 1 Corepressor by the Human Immunodeficiency Virus Type 1 Transactivator Induces Expression of Interleukin-2 and Its Receptor in T Cells. Mol. Cell. Biol. 25, 1620–1633. https://doi.org/10.1128/MCB.25.5.1620-1633.2005

Kwan, K.Y., Lam, M.M.S., Krsnik, Ž., Kawasawa, Y.I., Lefebvre, V., Šestan, N., 2008. SOX5 postmitotically regulates migration, postmigratory differentiation, and projections of subplate and deep-layer neocortical neurons. Proc. Natl. Acad. Sci. 105, 16021–16026. https://doi.org/10.1073/pnas.0806791105

Kwan, K.Y., Sestan, N., Anton, E.S., 2012. Transcriptional co-regulation of neuronal migration and laminar identity in the neocortex. Dev. Camb. Engl. 139, 1535–1546. https://doi.org/10.1242/dev.069963

Lai, T., Jabaudon, D., Molyneaux, B.J., Azim, E., Arlotta, P., Menezes, J.R.L., Macklis, J.D., 2008. SOX5 controls the sequential generation of distinct corticofugal neuron subtypes. Neuron 57, 232–247. https://doi.org/10.1016/j.neuron.2007.12.023

Leone, D.P., Heavner, W.E., Ferenczi, E.A., Dobreva, G., Huguenard, J.R., Grosschedl, R., McConnell, S.K., 2015a. Satb2 Regulates the Differentiation of Both Callosal and Subcerebral Projection Neurons in the Developing Cerebral Cortex. Cereb. Cortex 25, 3406–3419. https://doi.org/10.1093/cercor/bhu156

Leone, D.P., Heavner, W.E., Ferenczi, E.A., Dobreva, G., Huguenard, J.R., Grosschedl, R., McConnell, S.K., 2015b. Satb2 Regulates the Differentiation of Both Callosal and Subcerebral Projection Neurons in the Developing Cerebral Cortex. Cereb. Cortex N. Y. N 1991 25, 3406–3419. https://doi.org/10.1093/cercor/bhu156

Leone, D.P., Srinivasan, K., Chen, B., Alcamo, E., McConnell, S.K., 2008. The determination of projection neuron identity in the developing cerebral cortex. Curr. Opin. Neurobiol. 18, 28–35. https://doi.org/10.1016/j.conb.2008.05.006

Leoyklang, P., Suphapeetiporn, K., Siriwan, P., Desudchit, T., Chaowanapanja, P., Gahl, W.A., Shotelersuk, V., 2007. Heterozygous nonsense mutationSATB2 associated with cleft palate, osteoporosis, and cognitive defects. Hum. Mutat. 28, 732–738. https://doi.org/10.1002/humu.20515

Lewis, H., Samanta, D., Örsell, J.-L., Bosanko, K.A., Rowell, A., Jones, M., Dale, R.C., Taravath, S., Hahn, C.D., Krishnakumar, D., Chagnon, S., Keller, S., Hagebeuk, E., Pathak, S., Bebin, E.M., Arndt, D.H., Alexander, J.J., Mainali, G., Coppola, G., Maclean, J., Sparagana, S., McNamara, N., Smith, D.M., Raggio, V., Cruz, M., Fernández-Jaén, A., Kava, M.P., Emrick, L., Fish, J.L., Vanderver, A., Helman, G., Pierson, T.M., Zarate, Y.A., 2020. Epilepsy and Electroencephalographic Abnormalities in SATB2-Associated Syndrome. Pediatr. Neurol. 112, 94–100. https://doi.org/10.1016/j.pediatrneurol.2020.04.006

Lo, H., Ng, W., Fong, N., Lui, C.D., Lam, C., 2022. Novel finding of lissencephaly and severe osteopenia in a Chinese patient with *SATB2* -associated syndrome and a brief review of literature. Am. J. Med. Genet. A. 188, 2168–2172. https://doi.org/10.1002/ajmg.a.62732

Lozano, D., López, J.M., Jiménez, S., Morona, R., Ruíz, V., Martínez, A., Moreno, N., 2023. Expression of SATB1 and SATB2 in the brain of bony fishes: what fish reveal about evolution. Brain Struct. Funct. 228, 921–945. https://doi.org/10.1007/s00429-023-02632-z

Luo, L., Yang, F., Ding, J., Yan, D., Wang, D., Yang, S., Ding, L., Li, J., Chen, D., Ma, R., Wu, J., Tang, J., 2016. MiR-31 inhibits migration and invasion by targeting SATB2 in triple negative breast cancer. Gene 594, 47–58. https://doi.org/10.1016/j.gene.2016.08.057

Malatesta, P., Hartfuss, E., Gotz, M., 2000. Isolation of radial glial cells by fluorescent-activated cell sorting reveals a neuronal lineage. Development 127, 5253–5263. https://doi.org/10.1242/dev.127.24.5253

McConnell, S., 1988. Fates of visual cortical neurons in the ferret after isochronic and heterochronic transplantation. J. Neurosci. 8, 945–974. https://doi.org/10.1523/JNEUROSCI.08-03-00945.1988

McKenna, W.L., Betancourt, J., Larkin, K.A., Abrams, B., Guo, C., Rubenstein, J.L.R., Chen, B., 2011. Tbr1 and Fezf2 regulate alternate corticofugal neuronal identities during

neocortical development. J. Neurosci. Off. J. Soc. Neurosci. 31, 549–564. https://doi.org/10.1523/JNEUROSCI.4131-10.2011

McKenna, W.L., Ortiz-Londono, C.F., Mathew, T.K., Hoang, K., Katzman, S., Chen, B., 2015. Mutual regulation between Satb2 and Fezf2 promotes subcerebral projection neuron identity in the developing cerebral cortex. Proc. Natl. Acad. Sci. U. S. A. 112, 11702–11707. https://doi.org/10.1073/pnas.1504144112

Meers, M.P., Tenenbaum, D., Henikoff, S., 2019. Peak calling by Sparse Enrichment Analysis for CUT&RUN chromatin profiling. Epigenetics Chromatin 12, 42. https://doi.org/10.1186/s13072-019-0287-4

Minařík, M., Modrell, M.S., Gillis, J.A., Campbell, A.S., Fuller, I., Lyne, R., Micklem, G., Gela, D., Pšenička, M., Baker, C.V.H., 2023. Identification of multiple transcription factor genes potentially involved in the development of electrosensory versus mechanosensory lateral line organs (preprint). Developmental Biology. https://doi.org/10.1101/2023.04.14.536701

Miyata, T., Kawaguchi, A., Okano, H., Ogawa, M., 2001. Asymmetric Inheritance of Radial Glial Fibers by Cortical Neurons. Neuron 31, 727–741. https://doi.org/10.1016/S0896-6273(01)00420-2

Molyneaux, B.J., Arlotta, P., Hirata, T., Hibi, M., Macklis, J.D., 2005. Fezl Is Required for the Birth and Specification of Corticospinal Motor Neurons. Neuron 47, 817–831. https://doi.org/10.1016/j.neuron.2005.08.030

Molyneaux, B.J., Arlotta, P., Menezes, J.R.L., Macklis, J.D., 2007. Neuronal subtype specification in the cerebral cortex. Nat. Rev. Neurosci. 8, 427–437. https://doi.org/10.1038/nrn2151

Naik, R., Galande, S., 2019. SATB family chromatin organizers as master regulators of tumor progression. Oncogene 38, 1989–2004. https://doi.org/10.1038/s41388-018-0541-4

Nakagomi, K., Kohwi, Y., Dickinson, L.A., Kohwi-Shigematsu, T., 1994. A Novel DNA-Binding Motif in the Nuclear Matrix Attachment DNA-Binding Protein SATB1. Mol. Cell. Biol. 14, 1852–1860. https://doi.org/10.1128/mcb.14.3.1852-1860.1994

Neuroscience, 5th ed., 2012. , Neuroscience, 5th ed. Sinauer Associates, Sunderland, MA, US.

Noctor, S.C., Flint, A.C., Weissman, T.A., Dammerman, R.S., Kriegstein, A.R., 2001. Neurons derived from radial glial cells establish radial units in neocortex. Nature 409, 714–720. https://doi.org/10.1038/35055553

Patani, N., Jiang, W., Mansel, R., Newbold, R., Mokbel, K., 2009. The mRNA expression of SATB1 and SATB2 in human breast cancer. Cancer Cell Int. 9, 18. https://doi.org/10.1186/1475-2867-9-18

Peng, H., Xie, P., Liu, L., Kuang, X., Wang, Yimin, Qu, L., Gong, H., Jiang, S., Li, A., Ruan, Z., Ding, L., Yao, Z., Chen, C., Chen, M., Daigle, T.L., Dalley, R., Ding, Z., Duan, Y., Feiner, A., He, P., Hill, C., Hirokawa, K.E., Hong, G., Huang, L., Kebede, S., Kuo, H.-C., Larsen, R., Lesnar, P., Li, L., Li, Q., Li, X., Li, Yaoyao, Li, Yuanyuan, Liu, A., Lu, D., Mok, S., Ng, L., Nguyen, T.N., Ouyang, Q., Pan, J., Shen, E., Song, Y., Sunkin,

S.M., Tasic, B., Veldman, M.B., Wakeman, W., Wan, W., Wang, P., Wang, Q., Wang, T., Wang, Yaping, Xiong, F., Xiong, W., Xu, W., Ye, M., Yin, L., Yu, Y., Yuan, Jia, Yuan, Jing, Yun, Z., Zeng, S., Zhang, S., Zhao, S., Zhao, Z., Zhou, Z., Huang, Z.J., Esposito, L., Hawrylycz, M.J., Sorensen, S.A., Yang, X.W., Zheng, Y., Gu, Z., Xie, W., Koch, C., Luo, Q., Harris, J.A., Wang, Yun, Zeng, H., 2021. Morphological diversity of single neurons in molecularly defined cell types. Nature 598, 174–181. https://doi.org/10.1038/s41586-021-03941-1

Purbey, P.K., Singh, S., Kumar, P.P., Mehta, S., Ganesh, K.N., Mitra, D., Galande, S., 2008. PDZ domain-mediated dimerization and homeodomain-directed specificity are required for high-affinity DNA binding by SATB1. Nucleic Acids Res. 36, 2107–2122. https://doi.org/10.1093/nar/gkm1151

Qiu, S., Anderson, C.T., Levitt, P., Shepherd, G.M.G., 2011. Circuit-specific intracortical hyperconnectivity in mice with deletion of the autism-associated Met receptor tyrosine kinase. J. Neurosci. Off. J. Soc. Neurosci. 31, 5855–5864. https://doi.org/10.1523/JNEUROSCI.6569-10.2011

Rakic, P., 2009. Evolution of the neocortex: a perspective from developmental biology. Nat. Rev. Neurosci. 10, 724–735. https://doi.org/10.1038/nrn2719

Rakic, P., 1988. Specification of Cerebral Cortical Areas. Science 241, 170–176. https://doi.org/10.1126/science.3291116

Ripke, S., Neale, B.M., Corvin, A., Walters, J.T., Farh, K.-H., Holmans, P.A., Lee, P., Bulik-Sullivan, B., Collier, D.A., Huang, H., Pers, T.H., Agartz, I., Agerbo, E., Albus, M., Alexander, M., Amin, F., Bacanu, S.A., Begemann, M., Belliveau, R.A., Bene, J., Bergen, S.E., Bevilacqua, E., Bigdeli, T.B., Black, D.W., Bruggeman, R., Buccola, N.G., Buckner, R.L., Byerley, W., Cahn, W., Cai, G., Campion, D., Cantor, R.M., Carr, V.J., Carrera, N., Catts, S.V., Chambert, K.D., Chan, R.C., Chan, R.Y., Chen, E.Y., Cheng, W., Cheung, E.F., Chong, S.A., Cloninger, C.R., Cohen, D., Cohen, N., Cormican, P., Craddock, N., Crowley, J.J., Curtis, D., Davidson, M., Davis, K.L., Degenhardt, F., Del Favero, J., Demontis, D., Dikeos, D., Dinan, T., Djurovic, S., Donohoe, G., Drapeau, E., Duan, J., Dudbridge, F., Durmishi, N., Eichhammer, P., Eriksson, J., Escott-Price, V., Essioux, L., Fanous, A.H., Farrell, M.S., Frank, J., Franke, L., Freedman, R., Freimer, N.B., Friedl, M., Friedman, J.I., Fromer, M., Genovese, G., Georgieva, L., Giegling, I., Giusti-Rodríguez, P., Godard, S., Goldstein, J.I., Golimbet, V., Gopal, S., Gratten, J., de Haan, L., Hammer, C., Hamshere, M.L., Hansen, M., Hansen, T., Haroutunian, V., Hartmann, A.M., Henskens, F.A., Herms, S., Hirschhorn, J.N., Hoffmann, P., Hofman, A., Hollegaard, M.V., Hougaard, D.M., Ikeda, M., Joa, I., Julià, A., Kahn, R.S., Kalaydjieva, L., Karachanak-Yankova, S., Karjalainen, J., Kavanagh, D., Keller, M.C., Kennedy, J.L., Khrunin, A., Kim, Y., Klovins, J., Knowles, J.A., Konte, B., Kucinskas, V., Kucinskiene, Z.A., Kuzelova-Ptackova, H., Kähler, A.K., Laurent, C., Lee, J., Lee, S.H., Legge, S.E., Lerer, B., Li, M., Li, T., Liang, K.-Y., Lieberman, J., Limborska, S., Loughland, C.M., Lubinski, J., Lönnqvist, J., Macek, M., Magnusson, P.K., Maher, B.S., Maier, W., Mallet, J., Marsal, S., Mattheisen, M., Mattingsdal, M., McCarley, R.W., McDonald, C., McIntosh, A.M., Meier, S., Meijer, C.J., Melegh, B., Melle, I., Mesholam-Gately, R.I., Metspalu, A., Michie, P.T., Milani, L., Milanova, V., Mokrab, Y., Morris, D.W., Mors, O., Murphy, K.C., Murray, R.M., Myin-Germeys, I., Müller-Myhsok, B., Nelis, M., Nenadic, I., Nertney, D.A., Nestadt, G., Nicodemus, K.K., Nikitina-Zake, L., Nisenbaum, L., Nordin, A., O'Callaghan, E., O'Dushlaine, C., O'Neill, F.A., Oh, S.-Y., Olincy, A., Olsen, L., Van Os, J., Pantelis, C., Papadimitriou, G.N., Papiol, S., Parkhomenko, E., Pato, M.T.,

Paunio, T., Pejovic-Milovancevic, M., Perkins, D.O., Pietiläinen, O., Pimm, J., Pocklington, A.J., Powell, J., Price, A., Pulver, A.E., Purcell, S.M., Quested, D., Rasmussen, H.B., Reichenberg, A., Reimers, M.A., Richards, A.L., Roffman, J.L., Roussos, P., Ruderfer, D.M., Salomaa, V., Sanders, A.R., Schall, U., Schubert, C.R., Schulze, T.G., Schwab, S.G., Scolnick, E.M., Scott, R.J., Seidman, L.J., Shi, J., Sigurdsson, E., Silagadze, T., Silverman, J.M., Sim, K., Slominsky, P., Smoller, J.W., So, H.-C., Spencer, C.C.A., Stahl, E.A., Stefansson, H., Steinberg, S., Stogmann, E., Straub, R.E., Strengman, E., Strohmaier, J., Stroup, T.S., Subramaniam, M., Suvisaari, J., Svrakic, D.M., Szatkiewicz, J.P., Söderman, E., Thirumalai, S., Toncheva, D., Tosato, S., Veijola, J., Waddington, J., Walsh, D., Wang, D., Wang, Q., Webb, B.T., Weiser, M., Wildenauer, D.B., Williams, N.M., Williams, S., Witt, S.H., Wolen, A.R., Wong, E.H., Wormley, B.K., Xi, H.S., Zai, C.C., Zheng, X., Zimprich, F., Wray, N.R., Stefansson, K., Visscher, P.M., Adolfsson, R., Andreassen, O.A., Blackwood, D.H., Bramon, E., Buxbaum, J.D., Børglum, A.D., Cichon, S., Darvasi, A., Domenici, E., Ehrenreich, H., Esko, T., Gejman, P.V., Gill, M., Gurling, H., Hultman, C.M., Iwata, N., Jablensky, A.V., Jönsson, E.G., Kendler, K.S., Kirov, G., Knight, J., Lencz, T., Levinson, D.F., Li, Q.S., Liu, J., Malhotra, A.K., McCarroll, S.A., McQuillin, A., Moran, J.L., Mortensen, P.B., Mowry, B.J., Nöthen, M.M., Ophoff, R.A., Owen, M.J., Palotie, A., Pato, C.N., Petryshen, T.L., Posthuma, D., Rietschel, M., Riley, B.P., Rujescu, D., Sham, P.C., Sklar, P., St Clair, D., Weinberger, D.R., Wendland, J.R., Werge, T., Daly, M.J., Sullivan, P.F., O'Donovan, M.C., 2014. Biological Insights From 108 Schizophrenia-Associated Genetic Loci. Nature 511, 421–427. https://doi.org/10.1038/nature13595

Sahara, S., Yanagawa, Y., O'Leary, D.D.M., Stevens, C.F., 2012. The Fraction of Cortical GABAergic Neurons Is Constant from Near the Start of Cortical Neurogenesis to Adulthood. J. Neurosci. 32, 4755–4761. https://doi.org/10.1523/JNEUROSCI.6412-11.2012

satb2gene.org [WWW Document], n.d. . SATB2 Gene Found. URL https://satb2gene.org/ (accessed 7.31.23).

Sheehan-Rooney, K., Pálinkášová, B., Eberhart, J.K., Dixon, M.J., 2010. A cross-species analysis of Satb2 expression suggests deep conservation across vertebrate lineages. Dev. Dyn. 239, 3481–3491. https://doi.org/10.1002/dvdy.22483

Shepherd, G.M.G., 2005. Laminar and Columnar Organization of Ascending Excitatory Projections to Layer 2/3 Pyramidal Neurons in Rat Barrel Cortex. J. Neurosci. 25, 5670–5679. https://doi.org/10.1523/JNEUROSCI.1173-05.2005

Sills, J.A., Buckton, K.E., Raeburn, J.A., 1976. Severe mental retardation in a boy with partial trisomy 10q and partial monosomy 2q. J. Med. Genet. 13, 507–510. https://doi.org/10.1136/jmg.13.6.507

Skene, P.J., Henikoff, S., 2017. An efficient targeted nuclease strategy for high-resolution mapping of DNA binding sites. eLife 6, e21856. https://doi.org/10.7554/eLife.21856

Sokpor, G., Xie, Y., Rosenbusch, J., Tuoc, T., 2017. Chromatin Remodeling BAF (SWI/SNF) Complexes in Neural Development and Disorders. Front. Mol. Neurosci. 10.

Srinivasan, K., Leone, D.P., Bateson, R.K., Dobreva, G., Kohwi, Y., Kohwi-Shigematsu, T., Grosschedl, R., McConnell, S.K., 2012. A network of genetic repression and

derepression specifies projection fates in the developing neocortex. Proc. Natl. Acad. Sci. 109, 19071–19078. https://doi.org/10.1073/pnas.1216793109

Srivatsa, S., Parthasarathy, S., Britanova, O., Bormuth, I., Donahoo, A.-L., Ackerman, S.L., Richards, L.J., Tarabykin, V., 2014. Unc5C and DCC act downstream of Ctip2 and Satb2 and contribute to corpus callosum formation. Nat. Commun. 5, 3708. https://doi.org/10.1038/ncomms4708

Stiles, J., Jernigan, T.L., 2010. The Basics of Brain Development. Neuropsychol. Rev. 20, 327–348. https://doi.org/10.1007/s11065-010-9148-4

Su, Y., Wang, X., Yang, Y., Chen, L., Xia, W., Hoi, K.K., Li, H., Wang, Q., Yu, G., Chen, X., Wang, S., Wang, Y., Xiao, L., Verkhratsky, A., Fancy, S.P.J., Yi, C., Niu, J., 2023. Astrocyte endfoot formation controls the termination of oligodendrocyte precursor cell perivascular migration during development. Neuron 111, 190-201.e8. https://doi.org/10.1016/j.neuron.2022.10.032

Suter, B., 2010. Ephus: multipurpose data acquisition software for neuroscience experiments. Front. Neural Circuits 4. https://doi.org/10.3389/fncir.2010.00100

Szemes, M., Gyorgy, A., Paweletz, C., Dobi, A., Agoston, D.V., 2006. Isolation and Characterization of SATB2, a Novel AT-rich DNA Binding Protein Expressed in Development- and Cell-Specific Manner in the Rat Brain. Neurochem. Res. 31, 237. https://doi.org/10.1007/s11064-005-9012-8

Takahashi, T., Nowakowski, R.S., Caviness, V.S., 1995. The cell cycle of the pseudostratified ventricular epithelium of the embryonic murine cerebral wall. J. Neurosci. 15, 6046–6057. https://doi.org/10.1523/JNEUROSCI.15-09-06046.1995

Tang, W., Li, Y., Osimiri, L., Zhang, C., 2011. Osteoblast-specific Transcription Factor Osterix (Osx) Is an Upstream Regulator of Satb2 during Bone Formation. J. Biol. Chem. 286, 32995–33002. https://doi.org/10.1074/jbc.M111.244236

Tao, W., Zhang, A., Zhai, K., Huang, Z., Huang, H., Zhou, W., Huang, Q., Fang, X., Prager, B.C., Wang, X., Wu, Q., Sloan, A.E., Ahluwalia, M.S., Lathia, J.D., Yu, J.S., Rich, J.N., Bao, S., 2020. SATB2 drives glioblastoma growth by recruiting CBP to promote FOXM1 expression in glioma stem cells. EMBO Mol. Med. 12, e12291. https://doi.org/10.15252/emmm.202012291

Tasic, B., Yao, Z., Graybuck, L.T., Smith, K.A., Nguyen, T.N., Bertagnolli, D., Goldy, J., Garren, E., Economo, M.N., Viswanathan, S., Penn, O., Bakken, T., Menon, V., Miller, J., Fong, O., Hirokawa, K.E., Lathia, K., Rimorin, C., Tieu, M., Larsen, R., Casper, T., Barkan, E., Kroll, M., Parry, S., Shapovalova, N.V., Hirschstein, D., Pendergraft, J., Sullivan, H.A., Kim, T.K., Szafer, A., Dee, N., Groblewski, P., Wickersham, I., Cetin, A., Harris, J.A., Levi, B.P., Sunkin, S.M., Madisen, L., Daigle, T.L., Looger, L., Bernard, A., Phillips, J., Lein, E., Hawrylycz, M., Svoboda, K., Jones, A.R., Koch, C., Zeng, H., 2018. Shared and distinct transcriptomic cell types across neocortical areas. Nature 563, 72–78. https://doi.org/10.1038/s41586-018-0654-5

Taverna, E., Götz, M., Huttner, W.B., 2014. The cell biology of neurogenesis: toward an understanding of the development and evolution of the neocortex. Annu. Rev. Cell Dev. Biol. 30, 465–502. https://doi.org/10.1146/annurev-cellbio-101011-155801

The Nobel Prize in Physiology or Medicine 1906 [WWW Document], n.d. . NobelPrize.org. URL https://www.nobelprize.org/prizes/medicine/1906/summary/ (accessed 7.20.23).

Tissue expression of SATB2 - Summary - The Human Protein Atlas [WWW Document], n.d. URL https://www.proteinatlas.org/ENSG00000119042-SATB2/tissue (accessed 7.31.23).

Tsyporin, J., Tastad, D., Ma, X., Nehme, A., Finn, T., Huebner, L., Liu, G., Gallardo, D., Makhamreh, A., Roberts, J.M., Katzman, S., Sestan, N., McConnell, S.K., Yang, Z., Qiu, S., Chen, B., 2021. Transcriptional repression by FEZF2 restricts alternative identities of cortical projection neurons. Cell Rep. 35, 109269. https://doi.org/10.1016/j.celrep.2021.109269

Wang, Z., Yang, X., Chu, X., Zhang, J., Zhou, H., Shen, Y., Long, J., 2012. The structural basis for the oligomerization of the N-terminal domain of SATB1. Nucleic Acids Res. 40, 4193–4202. https://doi.org/10.1093/nar/gkr1284

Wang, Z., Yang, X., Guo, S., Yang, Y., Su, X.-C., Shen, Y., Long, J., 2014. Crystal Structure of the Ubiquitin-like Domain-CUT Repeat-like Tandem of Special AT-rich Sequence Binding Protein 1 (SATB1) Reveals a Coordinating DNA-binding Mechanism. J. Biol. Chem. 289, 27376–27385. https://doi.org/10.1074/jbc.M114.562314

Whitton, L., Apostolova, G., Rieder, D., Dechant, G., Rea, S., Donohoe, G., Morris, D.W., 2018. Genes regulated by SATB2 during neurodevelopment contribute to schizophrenia and educational attainment. PLoS Genet. 14, e1007515. https://doi.org/10.1371/journal.pgen.1007515

Yamasaki, K., Akiba, T., Yamasaki, T., Harata, K., 2007. Structural basis for recognition of the matrix attachment region of DNA by transcription factor SATB1. Nucleic Acids Res. 35, 5073–5084. https://doi.org/10.1093/nar/gkm504

Ye, J.-H., Xu, Y.-J., Gao, J., Yan, S.-G., Zhao, J., Tu, Q., Zhang, J., Duan, X.-J., Sommer, C.A., Mostoslavsky, G., Kaplan, D.L., Wu, Y.-N., Zhang, C.-P., Wang, L., Chen, J., 2011. Critical-size calvarial bone defects healing in a mouse model with silk scaffolds and SATB2-modified iPSCs. Biomaterials 32, 5065–5076. https://doi.org/10.1016/j.biomaterials.2011.03.053

Yu, G., Wang, L.-G., He, Q.-Y., 2015. ChIPseeker: an R/Bioconductor package for ChIP peak annotation, comparison and visualization. Bioinforma. Oxf. Engl. 31, 2382–2383. https://doi.org/10.1093/bioinformatics/btv145

Zarate, Y.A., Bosanko, K.A., Caffrey, A.R., Bernstein, J.A., Martin, D.M., Williams, M.S., Berry-Kravis, E.M., Mark, P.R., Manning, M.A., Bhambhani, V., Vargas, M., Seeley, A.H., Estrada-Veras, J.I., Dooren, M.F., Schwab, M., Vanderver, A., Melis, D., Alsadah, A., Sadler, L., Esch, H., Callewaert, B., Oostra, A., Maclean, J., Dentici, M.L., Orlando, V., Lipson, M., Sparagana, S.P., Maarup, T.J., Alsters, S.I., Brautbar, A., Kovitch, E., Naidu, S., Lees, M., Smith, D.M., Turner, L., Raggio, V., Spangenberg, L., Garcia-Miñaúr, S., Roeder, E.R., Littlejohn, R.O., Grange, D., Pfotenhauer, J., Jones, M.C., Balasubramanian, M., Martinez-Monseny, A., Blok, L.S., Gavrilova, R., Fish, J.L., 2019. Mutation update for the SATB2 gene. Hum. Mutat. 40, 1013–1029. https://doi.org/10.1002/humu.23771

Zarate, Y.A., Fish, J.L., 2017. SATB2-associated syndrome: Mechanisms, phenotype, and practical recommendations. Am. J. Med. Genet. A. 173, 327–337. https://doi.org/10.1002/ajmg.a.38022

Zarate, Y.A., Kalsner, L., Basinger, A., Jones, J.R., Li, C., Szybowska, M., Xu, Z.L., Vergano, S., Caffrey, A.R., Gonzalez, C.V., Dubbs, H., Zackai, E., Millan, F., Telegrafi, A., Baskin, B., Person, R., Fish, J.L., Everman, D.B., 2017. Genotype and phenotype in 12 additional individuals with SATB2-associated syndrome. Clin. Genet. 92, 423–429. https://doi.org/10.1111/cge.12982

Zeng, H., 2022. What is a cell type and how to define it? Cell 185, 2739–2755. https://doi.org/10.1016/j.cell.2022.06.031

Zhang, J., Tu, Q., Grosschedl, R., Kim, M.S., Griffin, T., Drissi, H., Yang, P., Chen, J., 2011. Roles of SATB2 in Osteogenic Differentiation and Bone Regeneration. Tissue Eng. Part A 17, 1767–1776. https://doi.org/10.1089/ten.tea.2010.0503

Zhang, X., Mennicke, C.V., Xiao, G., Beattie, R., Haider, M.A., Hippenmeyer, S., Ghashghaei, H.T., 2020. Clonal Analysis of Gliogenesis in the Cerebral Cortex Reveals Stochastic Expansion of Glia and Cell Autonomous Responses to Egfr Dosage. Cells 9, 2662. https://doi.org/10.3390/cells9122662

Zhang, Y., Liu, G., Guo, T., Liang, X.G., Du, H., Yang, L., Bhaduri, A., Li, X., Xu, Z., Zhang, Z., Li, Z., He, M., Tsyporin, J., Kriegstein, A.R., Rubenstein, J.L., Yang, Z., Chen, B., 2020. Cortical Neural Stem Cell Lineage Progression Is Regulated by Extrinsic Signaling Molecule Sonic Hedgehog. Cell Rep. 30, 4490-4504.e4. https://doi.org/10.1016/j.celrep.2020.03.027

Zhang, Z., Zhou, J., Tan, P., Pang, Y., Rivkin, A.C., Kirchgessner, M.A., Williams, E., Lee, C.-T., Liu, H., Franklin, A.D., Miyazaki, P.A., Bartlett, A., Aldridge, A.I., Vu, M., Boggeman, L., Fitzpatrick, C., Nery, J.R., Castanon, R.G., Rashid, M., Jacobs, M.W., Ito-Cole, T., O'Connor, C., Pinto-Duartec, A., Dominguez, B., Smith, J.B., Niu, S.-Y., Lee, K.-F., Jin, X., Mukamel, E.A., Behrens, M.M., Ecker, J.R., Callaway, E.M., 2021. Epigenomic diversity of cortical projection neurons in the mouse brain. Nature 598, 167–173. https://doi.org/10.1038/s41586-021-03223-w

Zhao, X., Qu, Z., Tickner, J., Xu, J., Dai, K., Zhang, X., 2014. The role of SATB2 in skeletogenesis and human disease. Cytokine Growth Factor Rev. 25, 35–44. https://doi.org/10.1016/j.cytogfr.2013.12.010